and then induction of DNA-fragmentations and apoptosis-like morphological changes follow (to be published elsewhere). However, it is not clear how activated RNase L leads to JNK phosphorylation. Once this new function of RNase L has been elucidated, novel targets for antitumor agents might emerge.

Recent literature shows that antibiotics (anisomycin, blasticidin S), ultraviolet-C, B, and α-sarcin can cause cleavage of cellular 28S rRNA, accompanying JNK phosphorylation. Thus, 28S rRNA cleavage seems to be associated with JNK phosphorylation [24–26]. Figures 3, 4 and 5 show that RNase L cleaves 28S rRNA in ECyd treated cells. These RNA fragments may act as mediator of the activation of JNK. Furthermore, other researchers proposed that activated RNase L not only cleaves RNA but also can interact with other proteins (RNase L-unknown protein(s) complex) through its C-terminal domain [27–29]. Such proteins associated with RNase L may be expected to be activated, and subsequently act for the phosphorylation of JNK.

In conclusion, our findings imply that RNase L is an essential member of apoptosis, triggered by impairment of RNA synthesis. RNase L-mediated apoptosis seems to be a pathway dependent on mitochondria. Understanding of this pathway further is expected to reveal a line of drug targets in the apoptotic mechanisms.

Acknowledgments The authors thank Dr. Hikoya Hayatsu (Faculty of Pharmaceutical Sciences, Okayama University) for helpful discussions. This research was partially supported by a grant for Exploractory Research (18659029, Y.W.) from the Ministry of Education, Culture, Sports, Science and Technology of Japan.

References

1. Shimamoto Y, Fujioka A, Kazuno H et al (2001) Antitumor activity and pharmacokinetics of TAS-106, 1-(3-*C*-ethynyl-β-D-*ribo*-pentofuranosyl) cytosine. Jpn J Cancer Res 92:343–351
2. Hattori H, Tanaka M, Fukushima M et al (1996) 1-(3-*C*-ethynyl-β-D-*ribo*-pentofuranosyl)-cytosine, 1-(3-*C*-ethynyl-β-D-*ribo*-pentofuranosyl)-uracil, and their nucleobase analogues as new potential multifunctional antitumor nucleosides with a broad spectrum of activity. J Med Chem 39:5005–5011
3. Takatori S, Kanda H, Takenaka K et al (1999) Antitumor mechanisms and metabolism of the novel antitumor nucleoside analogues, 1-(3-*C*-ethynyl-β-D-*ribo*-pentofuranosyl) cytosine and 1-(3-*C*-ethynyl-β-D-*ribo*-pentofuranosyl) uracil. Cancer Chemother Pharmacol 44:97–104
4. Takatori S, Tsutsumi S, Hidaka M et al (1998) The characterization of cell death induced by 1-(3-*C*-ethynyl-β-D-*ribo*-pentofuranosyl)-cytosine (ECyd) in FM3A cells. Nucleosides Nucleotides 17:1309–1317
5. Yoshimura A, Nakanishi M, Yatome C et al (2002) Comparative study on the biological properties of 2′, 5′-oligoadenylate derivatives with purified human RNase L expressed in *E. Coli*. J Biochem 132:643–648
6. Lesiak K, Torrence PF (1986) Synthesis and biological activities of oligo(8-bromoadenylates) as analogues of 5′-*O*-triphospho adenylyl(2′–5′)adenylyl (2′–5′) adenosine. J Med Chem 29:1015–1022
7. Ueno Y, Naito T, Kawada K et al (2005) Synthesis of novel siRNAs having thymidine dimers consisting of a carbamate or a urea linkage at their 3′ overhang regions and their ability to suppress human RNase L protein expression. Biochem Biophys Res Commun 330:1168–1175
8. Marzluff WF, Huang RCC (1984) Transcription of RNA in isolated nuclei Transcription and translation. IRL Press, Oxford (UK), pp 89–129
9. Chambon P (1975) Eukaryotic nuclear RNA polymerases. Annu Rev Biochem 44:613–638
10. Narcisi EM, Glover CV, Fechheimer M (1998) Fibrillarin, a conserved pre-ribosomal RNA processing protein of Giardia. J Eukaryot Microbiol 45:105–111
11. Chen M, Jiang P (2004) Altered subcellular distribution of nucleolar protein fibrillarin by actinomycin D in HEp-2 cells. Acta Pharmacol Sin 25:902–906
12. Michot B, Hassouna N, Bachellerie JP (1984) Secondary structure of mouse 28S rRNA and general model for the folding of the large rRNA in eukaryotes. Nucleic Acids Res 12:4259–4279
13. Han H, Schpartz A, Pellegrini M et al (1994) Mapping RNA regions in eukaryotic ribosomes that are accessible to methidium-propyl- EDTA.Fe(II) and EDTA.Fe(II). Biochemistry 33:9831–9844
14. Holmberg L, Melander Y, Nygard O (1994) Probing the conformational changes in 5.8S, 18S and 28S rRNA upon association of derived subunits into complete 80S ribosomes. Nucleic Acids Res 22:2776–2783
15. Dong B, Silverman RH (1995) 2–5A-dependent RNase molecules dimerize during activation by 2–5A. J Biol Chem 270:4133–4137
16. Stark GR, Kerr IM, Williams BR et al (1998) How cells respond to interferons. Annu Rev Biochem 67:227–264
17. Morten O, Christensen MO, Rene M et al (2004) Distinct effects of topoisomerase I and RNA polymerase I inhibitors suggest a dual mechanism of nucleolar/nucleoplasmic partitioning of topoisomerase I. J Biol Chem 279:21873–21882
18. Hartmann R, Nørby PL, Martensen PM et al (1998) Activation of 2′–5′ oligoadenylate synthetase by single-stranded and double-stranded RNA aptamers. J Biol Chem 273:3236–3246
19. Player MR, Torrence PF (1998) The 2–5A system: modulation of viral and cellular processes through acceleration of RNA degradation. Pharmacol Ther 78:55–113
20. Ugrinova I, Monier K, Ivaldi C et al (2007) Inactivation of nucleolin leads to nucleolar disruption, cell cycle arrest and defects in centrosome duplication. BMC Mol Biol 8:66
21. Iordanov MS, Paranjape JM, Zhou A et al (2000) Activation of p38 mitogen-activated protein kinase and c-Jun NH(2)-terminal kinase by double-stranded RNA and encephalomyocarditis virus: involvement of RNase L, protein kinase R, and alternative pathways. Mol Cell Biol 20:617–627
22. Malathi K, Paranjape JM, Ganapathi R et al (2004) HPC1/RNASEL mediates apoptosis of prostate cancer cells treated with 2′, 5′-oligoadenylates, topoisomerase I inhibitors, and tumor necrosis factor-related apoptosis-inducing ligand. Cancer Res 64:9144–9151
23. Li G, Xiang Y, Sabapathy K et al (2004) An apoptotic signaling pathway in the interferon antiviral response mediated by RNase L and c-Jun NH2-terminal kinase. J Biol Chem 279:1123–1131
24. Barr RK, Bogoyevitch MA (2001) The c-Jun N-terminal protein kinase family of mitogen-activated protein kinases (JNK MAPKs). Int J Biochem Cell Biol 33:1047–1063
25. Iordanov MS, Pribnow D, Magun JL et al (1997) Ribotoxic stress response: activation of the stress-activated protein kinase JNK1 by inhibitors of the peptidyl transferase reaction and by sequence-specific RNA damage to the α-sarcin/ricin loop in the 28S rRNA. Mol Cell Biol 17:3373–3381

26. Xia S, Li Y, Rosen EM et al (2007) Ribotoxic stress sensitizes glioblastoma cells to death receptor induced apoptosis: requirements for c-jun NH2-terminal kinase and Bim. Mol Cancer Res 5:783–792
27. Bettoun DJ, Scafonas A, Rutledge SJ et al (2005) Interaction between the androgen receptor and RNase L mediates a cross-talk between the interferon and androgen signaling pathways. J Biol Chem 280:38898–38901
28. Le RF, Salehzada T, Bisbal C et al (2005) A newly discovered function for RNase L in regulating translation termination. Nat Struct Mol Biol 12:505–512
29. Malathi K, Paranjape JM, Bulanova E et al (2005) A transcriptional signaling pathway in the IFN system mediated by 2′–5′-oligoadenylate activation of RNase L. Proc Natl Acad Sci USA 102:14533–14538

Biosci. Biotechnol. Biochem., **73** (1), 217–220, 2009

Note

Synthesis of Novel Conjugates of Tetraoxane Endoperoxide with Bis(Quaternary Ammonium Salts)

Naokazu KUMURA,[1] Hirotaka FURUKAWA,[1] Michiyo KOBAYASHI,[1] Arnold N. ONYANGO,[2] Minoru IZUMI,[1] Shuhei NAKAJIMA,[1] Hye-Sook KIM,[3] Yusuke WATAYA,[3] and Naomichi BABA[1,†]

[1]*Division of Bioscience, Graduate School of Natural Science and Technology, Okayama University, Tsushimanaka, Okayama 700-8530, Japan*
[2]*Department of Food Science and Postharvest Technology, Jomo Kenyatta University of Agriculture and Technology, P.O. Box 62000 Nairobi, Kenya*
[3]*Faculty of Pharmaceutical Science, Graduate School of Medicine, Dentistry and Pharmaceutical Science, Okayama University, Okayama 700-8530, Japan*

Received August 19, 2008; Accepted September 17, 2008; Online Publication, January 7, 2009
[doi:10.1271/bbb.80571]

Novel water-soluble conjugates of 1,2,4,5-tetraoxane bis(quaternary ammonium salts) were synthesized in a relatively stable crystalline form *via* four steps starting from methyltrioxorhenium-catalyzed endo-peroxidation of ethyl 4-oxocyclohexanecarboxylate with hydrogen peroxide in hexafluoro-2-propanol. The assay for the *in vitro* toxicity of water-soluble tetraoxanes 5a–5d to malaria parasites indicate that they were inactive against the *Plasmodium falciparum* FCR-3 strain.

Key words: tetraoxane; bis(quaternary ammonium salts); malaria; reactive oxygen species

Reactive oxygen species (ROS) have been well documented to be involved in cell signaling pathways regulating cell growth and cell death.[1] In higher concentrations, however, ROS interact with nucleic acids, proteins and polyunsaturated fatty acyl groups in lipids *via* covalent binding and redox reactions. Since ROS are generated by the decomposition of peroxides,[1–3] they have been considered as potential chemotherapeutic agents targeting malignant cells,[4–6] HIV viruses,[7] and malarial parasites.[8] The most well-known example is artemisinin (Scheme 1), a trioxane endoperoxide with antimalarial activity isolated from *Artemisia annua*.[8] The trioxane structure in this natural product is known to be essential for its antimalarial activity. Despite extensive studies, however, the mechanism for the activity of artemisinin is not fully understood.[9] Nevertheless, based on its structure-activity relationship, a variety of related peroxides have been synthesized[10–13] so far and their antimalarial activity has been assessed, creating potential candidates for new antimalarial medicines.

Bis(quaternary ammonium salts) interfere with the biosynthesis of phosphatidylcholine (PC), a major component of the cell membrane.[14] Based on this effect, bis(quaternary ammonium heterocycles) have been demonstrated to show antileukemic effectiveness.[15] Calas *et al.* have also demonstrated that interference with *de novo* PC biosynthesis by bis(quaternary ammonium salts) was lethal to malaria parasites, including chloroquine-resistant species (Scheme 1).[16] Therefore, if we combine these two components *via* covalent binding, the conjugate should have a different nature from the originals. For example, the solubility of the tetraoxane moiety in water may be significantly improved by the introduction of the ammonium ion. In addition to increasing water solubility, the conjugate may exhibit different biological and physiological properties. As described by Piantasosi *et al.*, the advantage of a combination of two or more biologically active components is due to the fact that each component has a different mechanism of action, and both of them have potential therapeutic activity.[17] Furthermore, the development of resistance to two bioactive drugs acquired by microorganisms, viruses, malignant cells and parasites may be reduced by the combination of the two components as a conjugate.[17] Such a combination may also reduce its mammal toxicity.[17] In fact, the incorporation of polar groups into endoperoxides has significantly reduced the neurotoxicity and superior antimalarial activity profiles.[18,19] Thus, in the present study, we undertook the first synthesis of novel conjugates of tetraoxane with bis(quaternary ammonium salts).

Due to the generally unstable nature of peroxide structures and difficulty in the purification of amphiphilic compounds, final compound **5** was synthesized according to Scheme 2 after a retrosynthetic analysis. With this synthetic route, basic intermediate peroxide **2** is modified stepwise to final compound **5** *via* ethyl ester hydrolysis, esterification with bromoalkanol, and substitution of the bromide with a tertiary amine by heating. Here, all the peroxides should be stable at least against the reaction conditions for quaternization of the nitrogen atom, usually by heating. The alkaline hydrolysis of **2** and re-esterification of **3** with bromoalkanols may not be difficult. As shown in Scheme 2, tetraoxane **2** was prepared according to the modified method of Iskara.[20] Treating ketone **1** with methyltrioxorhenium (VII) (MTO), 30% hydrogen peroxide and sulfuric acid in hexafluoro-2-propanol (HFIP) and subsequent quenching of the excess of hydrogen peroxide by adding manganase (IV) oxide (MnO_2) gave desired peroxide **2** in an 85% yield. Alkaline hydrolysis of peroxide **2** gave acid **3** in a quantitative yield. This acid was esterified with 2-bromoethanol or 3-bromopropanol to afford esters **4a** and **4b**, respectively. Quaternization of triethylamine or tripropylamine with bis(bromoesters) **4a** and

† To whom correspondence should be addressed. Tel: +81-86-251-8292; Fax: +81-86-251-8388; E-mail: babanaom@cc.okayama-u.ac.jp

4b requires the careful selection of a solvent for the optimum reaction rate, yield and crystallization of the products. Refluxing a mixture of **4a** and triethylamine in acetone for 18 h gave no desired ammonium salt **5a**. Refluxing for 20 h in EtOH resulted in a very low yield (<1%). On the other hand, refluxing for 14 h in acetonitrile afforded crystalline ammonium salt **5a** which was easily recrystallized from ether in a 28% yield. Fortunately, the peroxide did not decompose under this reaction. Similarly, acetonitrile was found to be the best solvent for the quaternization of triethylamine or tripropylamine with **4a** or **4b** to form **5a–5d**. Although almost pure **5a** and **5c** were obtained by recrystallization from a mixture of ethanol and ether, **5b** and **5d** did not crystallize and were purified by silica gel chromatography eluted with ($CHCl_3/CH_3OH/H_2O$: 65/15/2 → 65/35/4). Their chemical yields were not as high as those of the intermediates, since the quaternization reaction was not quantitative; the recovery of **5a** and **5c** from their recrystallization solvent was accompanied by some loss of them, and the recovery of **5b** and **5d** during the chromatographic purification was not complete due to their amphiphilic property. Their structure was confirmed as a red-colored spot on TLC by detection with the *N,N*-dimethyl-*p*-phenylenediammonium dichloride reagent that is specific for peroxides. Proton NMR and ESI MS also proved the purity and structural integrity. Thus, novel compounds **5a–5d** having the endoperoxide structure and bis(quaternary ammonium ions) in the same molecule were successfully synthesized. There are a number of biological systems to test the activity of **5a–5d**. In the present study, they were examined for their antimalarial activity in particular, since oxidative stress has been found to be a major causative factor to regulate malaria parasite growth and proliferation.

Tetraoxanes **5a–5d** were tested *in vitro* against the *P. falciparum* FCR-3 strain by following the protocol given in ref. 10. Briefly, asynchronously cultivated *P. falciparum* were used. Various concentrations of compounds in dimethylsulfoxide were prepared. Five microliters of each solution was added to individual wells of a 24-well maltidish. Erythrocytes with 0.3% parasitemia were added to each well containing 995 µl of the culture medium to give a final hematocrit level of 3%. The plates were incubated at 37 °C for 72 h in a CO_2–O_2–N_2 incubator (5% CO_2, 5% O_2, and 90% N_2 atmosphere). To evaluate the antimalarial activity of each test compound, we prepared thin blood films from each culture and stained them with Giemsa (E. Merck, Germany). A total of 1×10^4 erythrocytes per one thin blood film were examined by microscopy. All of the test compounds were assayed in duplicate at each concentration. Drug-free control cultures were run simultaneously. All data points represent the mean of three experiments. Parasitemia in the control was reaching between 4% and 5% after 72 h. The EC_{50} value refers to the concentration of the compound necessary to inhibit the increase in parasite density after 72 h by 50% of the control value. The assay results were as follows: **5a**, 100% growth (no growth inhibition) at 1.71×10^{-5} M; **5b**, 94% growth (4% inhibition) at 1.66×10^{-5} M; **5c**, 100% growth at 1.71×10^{-5} M; **5d**, 86% growth (14% inhibition) at 1.54×10^{-5} M. No morphological change of the infected erythrocytes was apparent in the application of **5a** at 1.71×10^{-5} M by the microscopic observation. The assay experiment indicated that all the quaternary aminium tetraoxanes were inactive against *P. falciparum*. Although the reason is unclear, their high water-solubility might have prevented effective interaction with the phospholipid bilayer of the malaria parasite cell membrane. Nevertheless, the novel bifunctional endoperoxides may exhibit new biological activity in different biological systems.

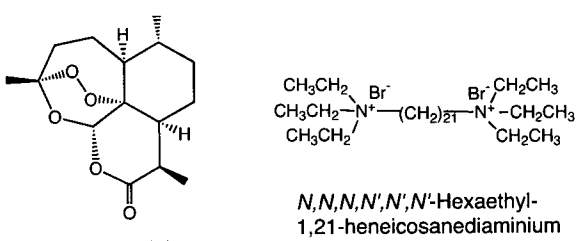

Scheme 1. Structure of Artemisinin and *N,N,N,N',N',N'*-Hexaethyl-1,21-heneicosanediaminium Dibromide.

Experimental

IR spectra were recorded by a Shimadzu IRPrestige-21 instrument, and NMR spectra were obtained with a Varian INOVA UNITY 600 (^1H, 600 MHz; ^{13}C, 150 MHz) spectrophotometer. ESI-MS data were collected with a Perkin Elmer API-III instrument in the positive ion mode with direct infusion.

Compound **2**. Methyltrioxorhenium (VII; 0.005 g, 0.02 mmol), 30% hydrogen peroxide (2.41 ml, 23.6 mmol) and sulfuric acid (0.634 ml,

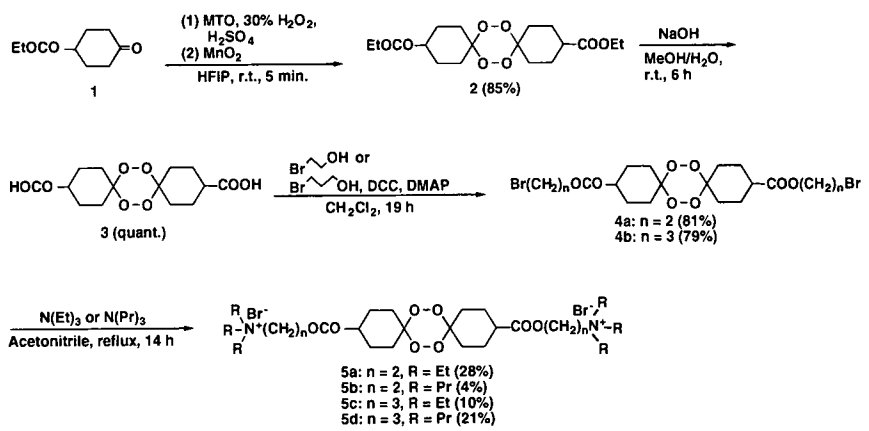

Scheme 2. Synthetic Scheme for Bis(quaternary ammonium salts) **5**.

11.9 mmol) were dissolved in HFIP (23 ml). To the solution was added ethyl 4-oxocyclohexanecarboxylate **1** (2.00 g, 11.8 mmol), and the mixture stirred at rt for 5 min. An excess of manganese (IV) oxide was then added, and stirring continued for an additional 15 min, before adding potassium carbonate (3.45 g, 25.0 mmol). The resulting mixture was filtered, and the solvent was evaporated under reduced pressure. The residue was purified by column chromatography on SiO_2, using hexane/ethyl acetate (7:3) as the eluent, to give **2** (85% yield). IR ν_{max} (KBr) cm^{-1}: 2937, 2870, 1724, 1465, 1444, 1398, 1381, 1355, 1319, 1255, 1192, 1184, 1138, 1064, 1022, 985, 939, 920, 864, 808, 759, 678, 553. NMR δ_H ($CDCl_3$): 1.24 (6H, t, J = 7.3 Hz, $-CH_3$ × 2), 1.52 (2H, br, cyclohexyl protons), 1.82 (12H, br, cyclohexyl protons), 2.39 (2H, m, cyclohexyl protons), 2.87 (2H, br, cyclohexyl protons), 4.12 (4H, q, J = 7.3 Hz, $-COOCH_2-$ × 2). NMR δ_C ($CDCl_3$): 14.17 ($-CH_3$), 23.72 (br), 24.59 (br), 28.01 (br), 30.27 (br), 41.56 (>*C*COO–), 60.42 ($-COOCH_2-$), 107.50 [>*C*(–O–O–)$_2$], 174.51 (–*C*OOEt); ESI-MS m/z: 390.18 $(M + NH_4)^+$.

Compound **3**. Alkaline hydrolysis was achieved by the usual method (quant). IR ν_{max} (KBr) cm^{-1}: 2943, 2872, 1691, 1463, 1423, 1342, 1319, 1220, 1136, 1066, 941, 914, 682, 555. NMR δ_H (CD_3OD): 1.54 (2H, br, cyclohexyl protons), 1.84 (12H, br, cyclohexyl protons), 2.40 (2H, m, cyclohexyl protons), 2.85 (2H, br, cyclohexyl protons). NMR δ_C (CD_3OD): 25.08 (br), 25.94 (br), 29.12 (br), 31.29 (br), 42.55 (>*C*COO–), 108.63 [>*C*(–O–O–)$_2$], 210.55 (–*C*OOH). ESI-MS m/z: 334.10 $(M + NH_4)^+$.

Compound **4**. The esterification of tetraoxane **3** with bromoalkanol was achieved by the DCC/DMAP method. **4a** (81% yield); IR ν_{max} (KBr) cm^{-1}: 2951, 2872, 1724, 1394, 1361, 1328, 1274, 1197, 1182, 1141, 1002, 974, 927, 657, 567. NMR δ_H ($CDCl_3$): 1.49 (2H, br, cyclohexyl protons), 1.75 (12H, br, cyclohexyl protons), 2.42 (2H, m, cyclohexyl protons), 2.80 (2H, br, cyclohexyl protons), 3.46 (4H, q, J = 5.9 Hz, $-CH_2Br$ × 2), 4.33 (4H, t, J = 5.9 Hz, $-COOCH_2-$ × 2). NMR δ_C ($CDCl_3$): 23.48 (br), 24.39 (br), 27.76 (br), 28.80 ($-CH_2Br$), 29.98 (br), 41.10 (>*C*COO–), 63.52 ($-COOCH_2-$), 107.23 [>*C*(–O–O–)$_2$], 173.76 ($-COOCH_2-$). ESI-MS m/z: 547.80 $(M + NH_4)^+$. **4b** (79% yield); IR ν_{max} (KBr) cm^{-1}: 2958, 2945, 2877, 1720, 1452, 1384, 1359, 1342, 1321, 1259, 1199, 1182, 1136, 1070, 1014, 975, 943, 925, 829, 650, 555. NMR δ_H ($CDCl_3$): 1.50 (2H, br, cyclohexyl protons), 1.75 (7H, br, cyclohexyl protons), 1.84 (3H, br, cyclohexyl protons), 1.91 (2H, br, cyclohexyl protons), 2.14 (4H, m, $-COOCH_2CH_2-$ × 2), 2.40 (2H, m, cyclohexyl protons), 2.83 (2H, br, cyclohexyl protons), 3.41 (4H, t, J = 6.6 Hz, $-CH_2Br$ × 2), 4.18 (4H, t, J = 5.9 Hz, $-COOCH_2-$ × 2). NMR δ_C ($CDCl_3$): 23.61 (br), 24.51 (br), 27.88 (br), 29.24 ($-CH_2Br$), 30.11 (br), 31.43 ($-COOCH_2CH_2-$), 41.40 (>*C*COO–), 62.04 ($-COOCH_2-$), 107.31 [>*C*(–O–O–)$_2$], 174.10 ($-COOCH_2-$). ESI-MS m/z: 576.00 $(M + NH_4)^+$.

Compound **5**. The synthesis of **5a–5d** was typically achieved by the reaction from **4a** to **5a**. Tetraoxane bromoester **4a** (0.55 g, 1.03 mmol) and distilled triethylamine (10 ml, 7.2 mmol) were dissolved in acetonitrile (20 ml) and refluxed for 14 h. The solvent was evaporated under reduced pressure, and the residue was washed with ether. Crystallization of the residue from a mixture of ethanol and diethyl ether gave desired bis(quaternary ammonium salt) **5a** (28% yield). IR ν_{max} (KBr) cm^{-1}: 2924, 2854, 1741, 1456, 1400, 1321, 1257, 1224, 1184, 1172, 1136, 1085, 1060, 999, 939, 786, 669, 555. NMR δ_H (CD_3OD): 1.33 [18H, t, J = 7.3 Hz, $-N(CH_2CH_3)_3$ × 2], 1.59 (2H, br, cyclohexyl protons), 1.74 (8H, br, cyclohexyl protons), 1.91 (2H, br, cyclohexyl protons), 1.96 (2H, br, cyclohexyl protons), 2.57 (2H, m, cyclohexyl protons), 2.92 (2H, br, cyclohexyl protons), 3.42 [12H, q, J = 7.3 Hz, $-N(CH_2CH_3)_3$ ×2], 3.63 (4H, t, J = 4.9 Hz, $-CH_2NEt_3$ × 2), 4.48 (4H, t, J = 4.9 Hz, $-COOCH_2-$ × 2). NMR δ_C (CD_3OD): 7.74 [$-N(CH_2CH_3)_3$], 25.04 (br), 25.87 (br), 28.99 (br), 31.17 (br), 42.55 (>*C*COO–), 54.65 [$-N(CH_2CH_3)_3$], 56.42 ($-CH_2NEt_3$), 58.47 ($-COOCH_2-$), 108.56 [>*C*(–O–O–)$_2$], 175.26 ($-COOCH_2-$). ESI-MS m/z: 286.20 $(M - 2Br)^{2+}$. **5b**: IR ν_{max} (KBr) cm^{-1}: 2926, 1732, 1473, 1456, 1396, 1384, 1359, 1319, 1257, 1195, 1178, 1138, 1066, 958. NMR δ_H (CD_3OD): 1.02 [18H, t, J = 7.3 Hz, $-N(CH_2CH_2CH_3)_3$ × 2], 1.58 (2H, br, cyclohexyl protons), 1.75 [20H, m, $-N(CH_2CH_2CH_3)_3$ × 2 and cyclohexyl protons], 1.93 (4H, br, cyclohexyl protons), 2.54 (2H, m, cyclohexyl protons), 2.91 (2H, m, cyclohexyl protons), 3.28 [12H, m, $-N(CH_2CH_2CH_3)_3$ × 2], 3.67 (4H, m, $-CH_2NPr_3$ × 2), 4.49 (4H, t, J = 3.9 Hz, $-COOCH_2-$ × 2). NMR δ_C (CD_3OD): 10.91 [$-N(CH_2CH_2CH_3)_3$], 16.55 [$-N(CH_2CH_2CH_3)_3$], 24.90 (br), 25.76 (br), 28.93 (br), 31.09 (br), 42.51 (>*C*COO–), 58.22 ($-COOCH_2-$), 58.68 ($-CH_2NPr_3$), 62.03 [$-N(CH_2CH_2CH_3)_3$], 109.50 [>*C*(–O–O–)$_2$], 175.24 ($-COOCH_2-$). ESI-MS m/z: 328.20 $(M - 2Br)^{2+}$. **5c**: IR ν_{max} (KBr) cm^{-1}: 2947, 2937, 1724, 1492, 1444, 1390, 1361, 1325, 1263, 1170, 1136, 1066, 999, 939, 920, 491. NMR δ_H (CD_3OD): 1.31 [18H, t, J = 7.3 Hz, $-N(CH_2CH_3)_3$ × 2], 1.57 (2H, br, cyclohexyl protons), 1.72 (6H, br, cyclohexyl protons), 1.82 (2H, br, cyclohexyl protons), 1.90 (4H, br, cyclohexyl protons), 2.07 (4H, m, $-COOCH_2CH_2-$ × 2), 2.54 (2H, m, cyclohexyl protons), 2.89 (2H, m, cyclohexyl protons), 3.30 (4H, m, $-COOCH_2CH_2-$ × 2), 3.36 [12H, q, J = 7.3 Hz, $-N(CH_2CH_3)_3$ × 2], 4.19 (4H, t, J = 6.1 Hz, $-COOCH_2-$ × 2). NMR δ_C (CD_3OD): 7.76 [$N(CH_2CH_3)_3$], 22.48 ($-COOCH_2CH_2-$), 25.01 (br), 25.88 (br), 29.09 (br), 31.18 (br), 42.54 (>*C*COO–), 54.01 [$-N(CH_2CH_3)_3$], 55.13 ($-CH_2NEt_3$), 62.28 ($-COOCH_2-$), 108.57 [>*C*(–O–O–)$_2$], 176.01 ($-COOCH_2-$). ESI-MS m/z: 300.20 $(M - 2Br)^{2+}$. **5d**: IR ν_{max} (KBr) cm^{-1}: 2974, 2943, 2881, 1724, 1489, 1473, 1458, 1388, 1319, 1197, 1180, 1062, 959, 642, 559. NMR δ_H (CD_3OD): 1.02 [18H, t, J = 7.3 Hz, $-N(CH_2CH_2CH_3)_3$ × 2], 1.58 (2H, br, cyclohexyl protons), 1.74 [20H, m, $-N(CH_2CH_2CH_3)_3$ × 2 and cyclohexyl protons], 1.91 (2H, br, cyclohexyl protons), 1.95 (2H, br, cyclohexyl protons), 2.10 (4H, m, $-COOCH_2CH_2-$ × 2), 2.57 (2H, m, cyclohexyl protons), 2.90 (2H, br, cyclohexyl protons), 3.27 [12H, m, $-N(CH_2CH_2CH_3)_3$ × 2], 3.40 (4H, m, $-CH_2NPr_3$ × 2), 4.19 (4H, t, J = 5.9 Hz, $-COOCH_2$ × 2). NMR δ_C (CD_3OD): 10.95 [$-N(CH_2CH_2CH_3)_3$], 16.48 [$-N(CH_2CH_2CH_3)_3$], 21.52 ($-COOCH_2CH_2-$), 24.99 (br), 25.81 (br), 29.06 (br), 31.17 (br), 42.48 (>*C*COO–), 56.94 ($-CH_2NPr_3$), 61.35 [$-N(CH_2CH_2CH_3)_3$], 62.33 ($-COOCH_2-$), 108.53 [>*C*(–O–O–)$_2$], 175.99 ($-COOCH_2-$). ESI-MS m/z: 342.10 $(M - 2Br)^{2+}$.

Acknowledgments

We thank Prof. Kenji Uneyama at Okayama University for his valuable advice with the present study. We are grateful to Central Glass Co., Ltd., for presenting HFIP. We also thank the staff in the laboratory of SC-NMR and the laboratory of API III mass spectrometry at Okayama University.

References

1) Thannickal, V. J., and Fanburg, B. L., Reactive oxygen species in cell signaling. *Am. J. Physiol. Lung Cell. Mol. Physiol.*, **279**, L1005–L1028 (2000).
2) Butler, A. R., Gilbert, B. C., Hulme, P., Irvine, L. R., Renton, L., and Whitwood, A. C., EPR evidence for the involvement of free radicals in the iron-catalyzed decomposition of Qinghaosu (artemisinin) and some derivatives; antimalarial action of some polycyclic endoperoxides. *Free Rad. Res.*, **28**, 471–476 (1998).
3) Opsenica, I., Terzić, N., Opsenica, D., Angelovski, G., Lehnig, M., Eilbracht, P., Tinant, B., Juranić, Z., Smith, K. S., Yang, Y. S, Diaz, D. S., Smith, O. L., Milhous, W. K., Doković, D., and Šolaja, B. A., Tetraoxane antimalarials and their reaction with Fe(II). *J. Med. Chem.*, **49**, 3790–3799 (2006).
4) Opsenica, D., Kyle, D. E., Milhous, W. K., and Šolaja, B. A., Antimalarial, antimycobacterial and antiproliferative activity of phenyl substituted mixed tetraoxanes. *J. Serb. Chem. Soc.*, **68**, 291–302 (2003).
5) Lai, H. Y., Sasaki, T., and Singh, N. P., Targeted treatment of cancer with artemisinin and artemisinin-tagged iron-carrying compounds. *Expert Opin. Ther. Targets*, **9**, 995–1007 (2005).
6) Terzić, N., Opsenica, D., Milie, D., Tinant, B., Smith, K. S., Milhous, W. K., and Šolaja, B. A., Deoxycholic acid-derived tetraoxane antimalarials and antiproliferatives. *J. Med. Chem.*, **50**, 5118–5127 (2007).
7) Jung, M., Lee, S., Kim, H., and Kim, H., Recent studies on natural products as anti-HIV agents. *Curr. Med. Chem.*, **7**, 649–661 (2000).
8) O'Neill, P. M., and Posner, G. H., A medicinal chemistry perspective on artemisinin and related endoperoxides. *J. Med. Chem.*, **47**, 2945–2964 (2004).

9) Stocks, P. A., Bray, P. G., Barton, V. E., Al-Hela, M., Jones, M., Araujo, N. C., Gibbons, P., Stephen, A. W., Hughes, R. H., Biagini, G. A., Davies, J., Amewu, R., Mercer, A. E., Ellis, G., and O'Neill, P. M., Evidence for a common non-heme chelatable-iron-dependent activation mechanism for semisynthetic and synthetic endoperoxide antimalarial drugs. *Angew. Chem.*, **119**, 6394–6399 (2007).

10) Kim, H. S., Shibata, Y., Wataya, Y., Tsuchiya, K., Masuyama, A., and Nojima, M., Synthesis and antimalarial activity of cyclic peroxides, 1,2,4,5,7-pentoxocanes and 1,2,4,5-tetroxanes. *J. Med. Chem.*, **42**, 2604–2606 (1999).

11) Tokuyasu, T., Masuyama, A., Nojima, M., McCullough, K. J., Kim, H.-S., and Wataya, Y., Yingzhaosu A analogues: synthesis by the ozonolysis of unsaturated hydroperoxides, structural analysis and determination of anti-malarial activity. *Tetrahedron*, **57**, 5979–5989 (2001).

12) Iskra, J., Danièle, B. D., and Begue, J. P., One-pot synthesis of non-symmetric tetraoxanes with the H_2O_2/MTO/fluorous alcohol system. *Tetrahedron Lett.*, **44**, 6309–6312 (2003).

13) Terent'v, A. O., Kutkin, A. V., Starikova, Z. A., Antipin, M. Y., Ogibin, Y. N., and Nikishin, G. I., New preparation of 1,2,4,5-tetraoxanes. *Synthesis*, **14**, 2356–2366 (2004).

14) Cain, B. F., Atwell, G. J., and Seelye, R. N., Potential antitumor agents. IX. bisquaternary salts. *J. Med. Chem.*, **11**, 963–966, and references therein to earlier papers (1968).

15) Hatfield, K. J., Olsnes, A. M., Gjertsen, B. T., and Bruserud, O., Antiangiogenic therapy in acute myelogenous leukemia: targeting of vascular endothelial growth factor and interleukin 8 as possible antileukemic strategies. *Curr. Cancer Drug Targets*, **5**, 229–248 (2005).

16) Calas, M., Ancelin, M. L., Cordina, G., Portefaix, P., Piquet, G., Vidal-Saihan, V., and Vial, H., Antimalarial activity of compounds interfering with *Plasmodium falciparum* phospholipid metabolism: comparison between mono- and bisquaternary ammonium salts. *J. Med. Chem.*, **43**, 505–516 (2000).

17) Parang, K., Wiebe, L. I., and Knaus, E. E., Novel approaches for designing 5′-O-ester prodrugs of 3′-azido-2′,3′-dideoxythymidine (AZT). *Curr. Med. Chem.*, **7**, 995–1039 (2000).

18) Haynes, R. K., From artemisinin to new artemisinin antimalarials: biosynthesis, extraction, old and new derivatives, stereochemistry and medicinal chemistry requirements. *Curr. Top. Med. Chem.*, **6**, 509–537 (2006).

19) Amewu, R., Stachulski, A. V., Ward, S. A., Berry, N. G., and Bray, P. G., Design and synthesis of orally active dispiro 1,2,4,5-tetraoxanes; synthetic antimalarials with superior activity to artemisinin. *Org. Biomol. Chem.*, **4**, 4431–4436 (2006).

20) Katja, Z., Stojan, S., Marko, Z., Danièle, B. D., and Iskra, J., Fluorinated alcohol directed formation of dispiro-1,2,4,5-tetraoxanes by hydrogen peroxide under acid conditions. *Tetrahedron*, **62**, 1479–1484 (2006).

Experimental Parasitology 121 (2009) 132–136

Contents lists available at ScienceDirect

Experimental Parasitology

journal homepage: www.elsevier.com/locate/yexpr

Toxoplasma gondii: A simple high-throughput assay for drug screening *in vitro*

ChunMei Jin [a], Kusuma Kaewintajuk [a], JingHua Jiang [a], WooJin Jeong [a], Masaki Kamata [b], Hye-Sook KIM [c], Yusuke Wataya [c], Hyun Park [a,*]

[a] Department of Infection Biology, Zoonosis Research Center, Wonkwang University School of Medicine, 344-2, Shinyong-dong, Iksan, Chonbuk 570-749, Republic of Korea
[b] Department of Chemistry, Faculty of Education Niigata University, Ikarashi, Niigata 950-2181, Japan
[c] Faculty of Pharmaceutical Sciences, Okayama University, Tsushima, Okayama 700-8530, Japan

ARTICLE INFO

Article history:
Received 20 February 2008
Received in revised form 6 October 2008
Accepted 8 October 2008
Available online 17 October 2008

Keywords:
Toxoplasma gondii drug screening system
Trypan blue dye
MTS method
LDH assay

ABSTRACT

Toxoplasma gondii is the etiologic agent of toxoplasmosis. Although the combination of sulfadiazine and pyrimethamine is used as therapy for this disease, these drugs can have serious side effects and its use is limited in pregnancy. Therefore there is a need for new anti-*T. gondii* drugs in the clinic. Some systems for *T. gondii* drug screening have been described, but these have limitations and can be difficult. In order to solve these problems, we established a system to screen drugs *in vitro* that involved using cell viability methods to calculate drug selectivities, which are Trypan blue, [3-(4,5-dimethylthiazol-zyl)-5-(3-carboxymethoxyphenyl)-2-(4-sulfophenyl)-2H-tetrazoliuzolium, inner salt] (MTS) method and lactate dehydrogenase (LDH) assay. These assays were simple to establish and perform. The IC_{50} values calculated from the morphological assay were not significantly different from the EC_{50} values calculated using the other three methods. In particular, the results of the morphological assay showed a distinct association with the MTS assay ($R = 0.9841$). These assays could be used for a wide range of applications in the screening of new drugs and may provide an alternative to the techniques currently used to screen for candidate anti-*T. gondii* compounds *in vitro*. In this study, we also tested many compounds and identified some that had a good anti-*T. gondii* effect *in vitro* based on the MTS assay. This simple and fast system allowed us to determine which compounds to investigate further using *in vivo* experiments.

1. Introduction

Toxoplasma gondii is a unicellular obligate intracellular parasite, closely related to other medically important protozoan parasites, such as Plasmodium and Cryptosporidium, in the phylum Apicomplexa. *T. gondii* is the etiologic agent of toxoplasmosis which is a serious medical problem worldwide. Although the combination of pyrimethamine and sulfadiazine remains the mainstay for the treatment of *T. gondii*-induced diseases, it is not recommended for the treatment of acute toxoplasmosis in pregnancy and in AIDS patients (Haverkos, 1987). Therefore, new therapeutic anti-*T. gondii* drugs with good efficacy and lower toxicity are urgently needed.

The morphological assay is a visual method for screening drugs that is simple but also requires a significant amount of labor. Some other systems for *T. gondii* drug screening have also been developed. *In vitro* methods used to evaluate a compound's anti-toxoplasma activity include growth assays and enzymatic assays. Parasites can also be measured by the incorporation of radioactive uracil (Pfefferkorn and Pfefferkorn, 1977), by *T. gondii*-specific antibodies in an ELISA (Derouin and Chastang, 1998; Merli et al., 1985), by transgenic expression of the bacterial β-galactosidase reporter gene (McFadden et al., 1997), or by a FACS-based assay or yellow fluorescent protein assay (Gay-Andrieu et al., 1999; Gubbels et al., 2003). These have their advantages but also their limitations, such as the use of radioactive compounds, expensive instruments and agents. The aim of this study was to develop an *in vitro* screening system that was not only easy to establish and perform, but also produced results similar to the morphological assay, and to screen for candidate anti-*T. gondii* drugs using this system.

2. Materials and methods

2.1. Chemicals

Sulfadiazine, pyrimethamine and spiramycin were purchased from Sigma Chemical Company (St. Louis, MO, USA). CellTiter 96® AQ_{ueous} One Solution Cell Proliferation Assay kit and CytoTox 96® Assay kit were purchased from Promega Corporation (Madison, WI, USA). Synthetic endoperoxides were prepared according to the procedures reported by Kamata et al. (2002, Japan). All sera, antibiotics and RPMI 1640 for cell culture were obtained from Invitrogen (Grand Island, NY, USA). All other chemicals were of reagent grade.

* Corresponding author. Fax: +82 63 857 0342.
E-mail address: hyunpk@wonkwang.ac.kr (H. Park).

0014-4894/$ - see front matter © 2008 Elsevier Inc. All rights reserved.
doi:10.1016/j.exppara.2008.10.006

2.2. Cell culture and T. gondii

HeLa and MDBK cells were cultured in RPMI medium 1640 supplemented with 10% heat-inactivated fetal bovine serum, 100 units/ml penicillin and 100 μl/ml streptomycin with 5% CO_2 at 37 °C. *T. gondii* (RH strain) was maintained in ICR mice (Daehan Biolink Co., Korea) and tachyzoites were obtained from peritoneal fluids.

2.3. Morphology assay

The infection ratio of host cells were measured by conventional Giemsa staining. Briefly, cells were infected with *T. gondii* (host cell:tachyzoites = 1:5) for 24 h in 24-well plates (the cells were put on a glass cover in each well in advance), and then treated with drugs. After 24 h, the medium was discarded and the glass cover was rinsed three times with phosphate-buffered saline (PBS) solution, fixed in methanol for 5 min and stained with Giemsa solution for 15 min; the slides were then dried and the cells were counted using an oil objective.

2.4. Trypan blue dye test

To assay the viability of host cells, the Trypan blue dye test was performed as described by Tanaka et al. (1995). Briefly, cells were infected with *T. gondii* for 24 h in 24-well plates, treated with drugs, stained with Trypan blue dye, and then counted using a haemocytometer. Cells excluding Trypan blue were considered viable.

2.5. ELISA for MTS assay

The MTS assay is a colorimetric method for determining the number of viable cells using the CellTiter 96® AQ_{ueous} One Solution Cell Proliferation Assay kit (Cory et al., 1991; Riss and Moravec, 1992). This assay measures dehydrogenase enzymes in metabolically active cells (Berridge and Tan, 1993). HeLa cells were grown and infected with *T. gondii* for 24 h in 96-well microplates and then treated with drugs for 24 h, MTS solution (20 μl) was added directly into the culture wells and incubated for 1.5 h at 37 °C. The absorbance at 490 nm was then recorded in an ELISA microplate reader. Cell viability was expressed as a percent of the control value.

2.6. LDH assay for cytotoxicity

The lactate dehydrogenase (LDH) activity was measured by the CytoTox 96® Assay kit (Korzeniewski and Callewaert, 1983; Decker and Lohmann-Matthes, 1988). The cell treatment and infection steps in this assay were similar to those in the MTS assay. Sample supernatants (50 μl) were transferred to a fresh 96-well plate, reconstituted Substrate Mix (50 μl) was added to each supernatant sample, and the enzymatic reaction was allowed to proceed for 30 min at room temperature in the dark. The enzymatic activity was then stopped by adding 50 μl/well of stop solution. The absorbance at 490 nm was then measured using an ELISA plate reader. The number of cells present is directly proportional to the absorbance.

2.7. Statistical analysis

Student's *t*-test was performed for statistical analysis. All data were presented as means ± SD of at least three of four experiments. Individual inhibitory concentrations (IC_{50}) and individual effective concentrations (EC_{50}) were determined. Standard correlation analysis was used to establish association between IC_{50} values and EC_{50} values obtained from different assays with various drugs. For each compound, the selectivity was calculated by the formula: selectivity = HeLa cell EC_{50}/*T. gondii* EC_{50}. These data reflected the efficacy of a compound against *T. gondii*.

3. Results and discussion

In order to confirm the cell viability assay as a drug screening tool, the relationship between the morphological assay and the Trypan blue, MTS and LDH assays was explored.

First, the data obtained from these four assays after treatment with the standard anti-toxoplasma medications, sulfadiazine, pyrimethamine and spiramycin, were analyzed by linear regression analysis (Figs. 1–4). Both the inhibition of infected host cells and cell viability were reduced in a concentration-dependent manner. A good fit of the data was observed with all regressions (all regressions resulted in correlation coefficients higher than 0.9).

Then, by correlation analysis, IC_{50} and EC_{50} values were compared for these four *in vitro* methods. For sulfadiazine in *T. gondii*-infected HeLa cells, the IC_{50} value based on the morphological assay was 6.89 mM, which was not statistically different from

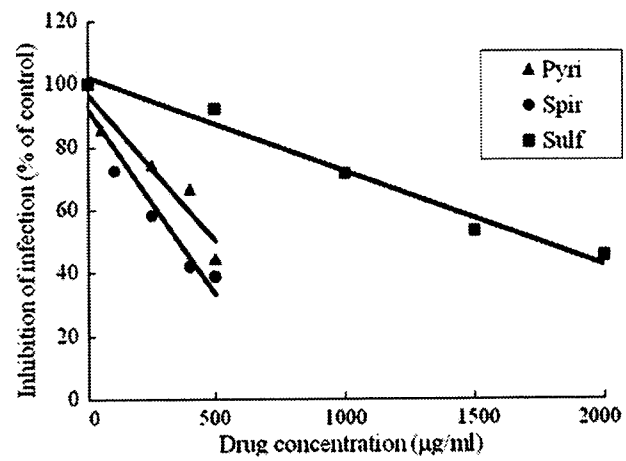

Fig. 1. Inhibitory effect of sulfadiazine (Sulf; $R = 0.9885$), pyrimethamine (Pyri; $R = 0.9732$) and spiramycin (Spir; $R = 0.9631$) in *T. gondii*-infected HeLa cells by giemsa strain (morphology) assay.

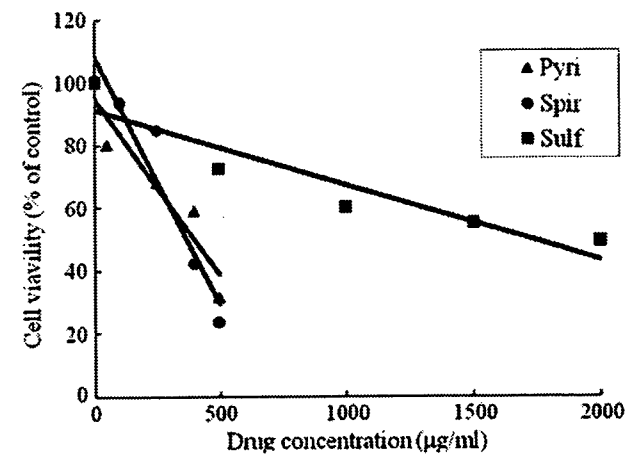

Fig. 2. Trypan blue assay of cell viability of *T. gondii*-infected HeLa cells after treatment with sulfadiazine (Sulf; $R = 0.9341$), pyrimethamine (Pyri; $R = 0.9700$) and spiramycin (Spir; $R = 0.9593$).

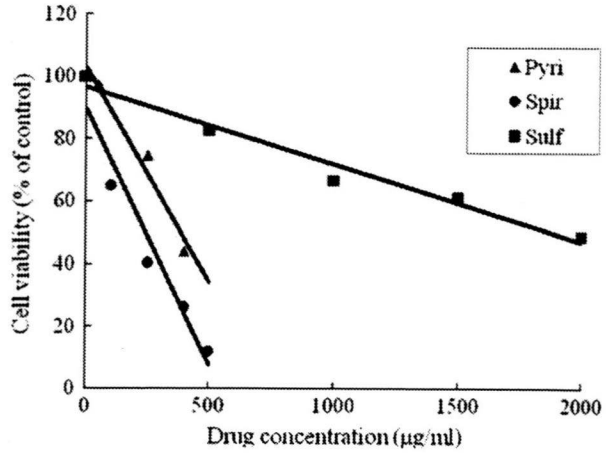

Fig. 3. LDH assay of cell viability of *T. gondii*-infected HeLa cells after treatment with sulfadiazine (Sulf; $R = 0.9853$), pyrimethamine (Pyri; $R = 0.9805$) and spiramycin (Spir; $R = 0.9661$).

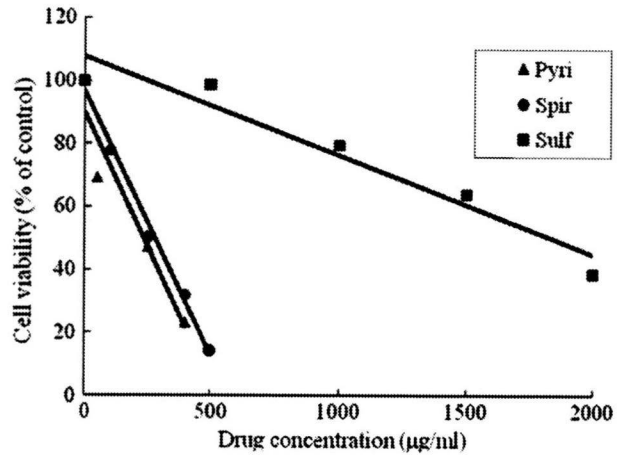

Fig. 4. MTS assay of cell viability of *T. gondii*-infected HeLa cells after treatment with sulfadiazine (Sulf; $R = 0.9688$), pyrimethamine (Pyri; $R = 0.9735$) and spiramycin (Spir; $R = 0.9843$).

Table 1
Comparison of IC_{50} values from the morphological assay and EC_{50} values from Trypan blue dye, LDH and MTS assays in HeLa cells.

Drugs	Morphological assay IC_{50}	Trypan blue dye EC_{50}	LDH assay EC_{50}	MTS assay EC_{50}
Sulf (mM)	6.89 ± 0.24	5.74 ± 1.97	5.91 ± 2.39	7.96 ± 0.79
Pyri (mM)	0.75 ± 0.48	0.69 ± 0.42	0.54 ± 0.29	0.85 ± 0.35
Spir (μg/ml)	307 ± 73	318 ± 82	128 ± 59*	247 ± 106

Sulf, sulfadiazine; Pyri, pyrimethamine; Spir, spiramycin.
* $P < 0.05$ ($n = 3$).

the EC_{50} values for the other three methods, being 5.74, 5.91 and 7.96 mM, for Trypan blue, MTS and LDH, respectively. For pyrimethamine in HeLa cells, the EC_{50} values from the Trypan blue, LDH and MTS assays were not significantly different from IC_{50} value of the morphology assays. For spiramycin, the EC_{50} of the LDH assay was significantly lower than the IC_{50} value ($P < 0.05$), while

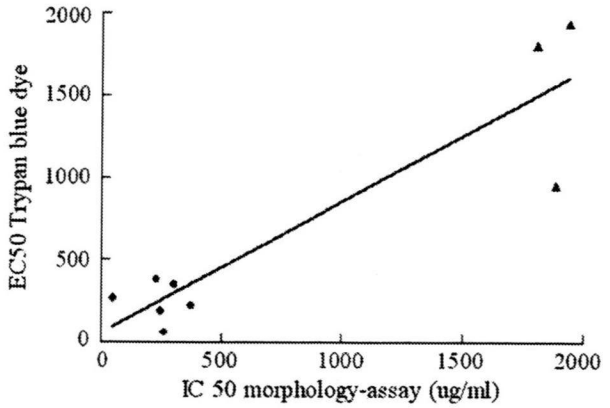

Fig. 5. Scatter plot for the association of individual IC_{50} and EC_{50} values for sulfadiazine (FW: 272.3, triangles), pyrimethamine (FW: 248.7, diamonds) and spiramycin (circles) determined by morphology assay and Trypan blue assay ($n = 3$, $R = 0.8865$).

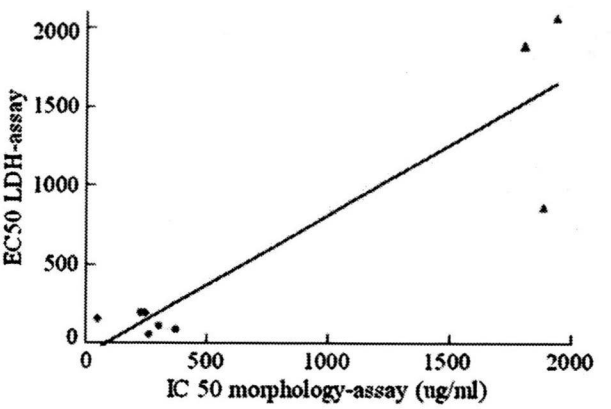

Fig. 6. Scatter plot for the association of individual IC_{50} and EC_{50} values for sulfadiazine (FW: 272.3, triangles), pyrimethamine (FW: 248.7, diamonds) and spiramycin (circles) determined by morphology assay and LDH assay ($n = 3$, $R = 0.7841$).

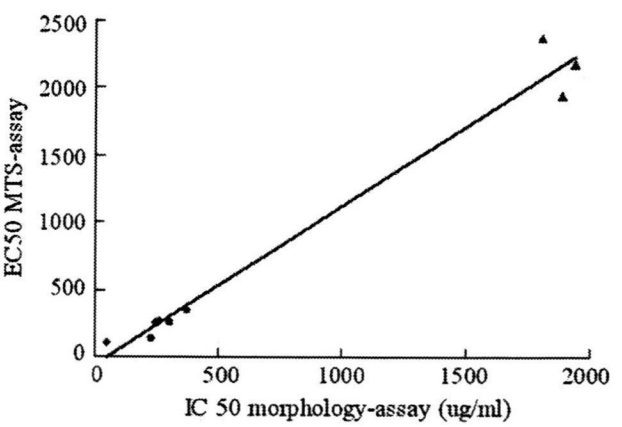

Fig. 7. Scatter plot for the association of individual IC_{50} and EC_{50} values for sulfadiazine (FW: 272.3, triangles), pyrimethamine FW: 248.7, diamonds) and spiramycin (circles) determined by morphology assay and MTS assay ($n = 3$, $R = 0.9841$).

the EC_{50} values of the Trypan blue and MTS assays were not significantly different from the morphology IC_{50} value (Table 1). Another

cell line, MDBK cells, was also used to establish this relationship. In this cell line, the IC_{50} values from the morphological assay were not significantly different from the EC_{50} values calculated using the other three methods (data not shown).

Furthermore, the EC_{50} values obtained from the Trypan blue, LDH and MTS assays were compared separately to the IC_{50} values from the morphological assay by correlation analysis. Graphs illustrating the data are shown in Figs. 5–7. The results from the morphological assay showed an association with Trypan blue (Fig. 5, $R = 0.8865$), LDH assay (Fig. 6. $R = 0.7841$) and MTS assay (Fig. 7, $R = 0.9841$), respectively.

The current *in vitro* methods used to evaluate anti-toxoplasma activity of a compound include growth assays and enzymatic assays (Bunetel et al., 1995; Chio and Queener, 1993; Derouin and Chastang, 1988; Iltzsch et al., 1995; Mack and McLeod, 1984; Pfefferkorn et al., 1992). In 1997, McFadden developed a strain of *T. gondii* that expressed bacterial β-galactosidase, which provided a high-throughput and nonradioactive alternative for the identification of anti-*T. gondii* compounds. Gubbels et al. (2003) introduced a high-throughput growth assay based on a highly fluorescent transgenic parasite line. However, all of these assays involve the use of expensive reagents, multiple manipulations or radiolabelled compounds (McFadden et al., 1997). The morphological assay is a method for observing *T. gondii*-infected host cells and can be used to screen drugs. It requires little technical equipment, but is labor-intensive and requires highly trained personnel. One aim of this study was to find a simple and practical method for screening anti-*T. gondii* drugs *in vitro*. In our studies, the infection ratio of host cells was measured by the morphological assay. Trypan blue, LDH and MTS assays were used to test the viability of host cells in these experiments which closely paralleled in the results of morphological assay and provide a simple method for quantification of anti-*T. gondii* drug activity. They combine the advantages of the morphological assay and overcome its disadvantages. Even though we thought initially that all three methods might be used instead of the morphological assay, the Trypan blue assay required greater cell numbers than the other two methods. After treatment with spiramycin, the LDH assay was only slightly significant and had the lowest R value ($R = 0.7841$). Thus, among these three methods, the MTS assay was closest to the morphological assay in performance and had the highest R value ($R = 0.9841$).

The MTS assay is similar to the MTT (3-(4,5-Dimethyl-2-thiazolyl)-2,5-di-phenyl-2 H-tetrazolium bromide) assay. These assays can both be performed in multi-well plates with no washing or cell harvesting steps, but the MTS assay does not require a volatile organic solvent to solubilize the formazan product and is therefore safer to perform. To determine whether these methods could be used on other cell lines, the same experiments were performed in MDBK cells. The results of the morphological assay were not significantly different from those for the other three methods, and therefore the MTS assay and HeLa cells were chosen for screening drugs in this study.

Table 2
The selectivity of sulfadiazine, pyrimethamine and spiramycin by MTS assay in HeLa cells.

	HeLa cell EC_{50}	*T. gondii* EC_{50}	Selectivity[a]
Sulf (mM)	6.13	7.96	0.8
Pyri (mM)	0.76	0.85	0.9
Spir (μg/ml)	253	247	1.0

Sulf, sulfadiazine; Pyri, pyrimethamine; Spir, spiramycin.
[a] Selectivity = HeLa cell EC_{50}/*T. gondii* EC_{50}.

Table 3
Compounds with anti-*T. gondii* activity in HeLa cells.

Name of compound	HeLa cell EC_{50}[a] (μM)	*T. gondii* EC_{50}[a] (μM)	Selectivity	*T. gondii* IC_{50}[b] (μM)
62 (1,5-bis(4-methoxyphenyl)-6,7-dioxabicyclo [3.2.2]nonane)	57.1	11.7	4.9	26.6
98 (1,5-bis(4-fluorophenyl)-6,7-dioxabicyclo[3.2.2] nonane)	45.9	11.9	3.9	8.9

[a] Using MTS assay; all data were measured in triplicate.
[b] Using morphological assay, $n = 3$.

The selectivities of sulfadiazine, pyrimethamine and spiramycin are listed in Table 2; being 0.8, 0.9 and 1.0, respectively. Based on the above data, if the selectivity of other chemicals were more than 1.0, we considered that such drugs would have an anti-*T. gondii* effect and low toxicity in HeLa cells.

Artemisinins contain an endoperoxide bridge that is essential for antimalarial activity and appears to undergo iron-catalyzed decomposition into free radicals (Meshnick, 2001). Artemisinin analogs are proven antimalarials, although they are fairly expensive to produce, in part because they are semi-synthetic plant products (Abdin et al., 2003). The naturally occurring 1,2,4-trioxane artemisinin and artemisinin derivatives such as artemether, which was originally developed to treat malaria, have the ability to inhibit toxoplasma replication *in vitro* (Berens et al., 1998; Chang et al., 1989; Holfels et al., 1994; Ou-Yang et al., 1990). Four derivatives of artemisinin also inhibited the replication of *T. gondii* in cell culture (Jones-Brando et al., 2006). We therefore tested more than 300 compounds from Japan that had an endoperoxide ring structure and antimalarial effects to determine whether they had anti-*T. gondii* activity based on the MTS method. More than 50 of these compounds had a selectivity of higher than 1.0 (the identity of most of these compounds cannot currently be revealed because of patent issues). Among them, compounds No.62 (1,5-bis(4-methoxyphenyl)-6,7-dioxabicyclo [3.2.2]nonane) and No.98 (1,5-bis(4-fluorophenyl)-6,7-dioxabicyclo[3.2.2]nonane) showed good anti-*T. gondii* activity, and their selectivities were all higher than 3.5 (Table 3). We then tested these two compounds in the morphological assay and found that they inhibited *T. gondii* infection in HeLa cells. The IC_{50} values were 26.6 and 8.9 μM, respectively (Table 3), and were not significantly different from the EC_{50} values calculated from the MTS assay. These results showed that this simple system could be used to screen the anti-*T. gondii* drugs *in vitro*. The activity of these anti-apicomplexa drugs and related compounds should be verified using *in vivo* animal models and their clinical availability further confirmed.

In conclusion, we have investigated several methods to determine their utility for screening candidate anti-*T. gondii* drugs *in vitro*. The results of Trypan blue, MTS and LDH assays efficiently reflected the results of the morphological assay, and the MTS and Trypan blue assays were more sensitive than the LDH assay. Furthermore, the MTS assay was fast and simple to establish, easy to perform with simple calculations, and required only small amounts of chemicals. In HeLa and MDBK cells, the selectivity was high, so we believe that these three methods could be used in other cell lines to screen large numbers of compounds for anti-*T. gondii* effects and may offer a solution to the technical difficulties of *T. gondii* screening *in vitro*.

We also tested many endoperoxide ring structure compounds using this screening system and found that some of them had a good anti-*T. gondii* effect *in vitro*. Based on these *in intro* findings, we will further investigate the mechanism of these compounds through *in vivo* animal experiments.

Acknowledgments

We thank Dr. Myoung-Hee Ahn, Dr. Jae-Sook Ryu and Han-Kyu Choi for teaching us the techniques.

This work was supported by the Korea Foundation for International Cooperation of Science and Technology (KICOS) through a grant provided by the Korean Ministry of Science and Technology (MOST) in No. 2007-00208 and by Grant No. RTI05-03-02 from the Regional Technology Innovation Program of Ministry of Commerce, Industry and Energy (MOCIE), Korea.

References

Abdin, M.Z., Israr, M., Rehman, R.U., Jain, S.K., 2003. Artemisinin, a novel antimalarial drug: biochemical and molecular approaches for enhanced production. Planta Medica 69, 289–299.

Berens, R.L., Krug, E.C., Nash, P.B., Curiel, T.J., 1998. Selection and characteriza-tion of *Toxoplasma gondii* mutants resistant to artemisinin. Journal of infectious diseases 177, 1128–1131.

Berridge, M.V., Tan, A.S., 1993. Characterization of the cellular reduction of 3-(4,5-dimethylthiazol-2-yl)-2,5-diphenyltetrazolium bromide (MTT): subcellular localization, substrate dependence, and involvement of mitochondrial electron transport in MTT reduction. Archives of Biochemistry and Biophysics 303, 474–482.

Bunetel, L., Guerin, J., Andre, P., Robert, R., Deunff, J., 1995. Calibration of an in vitro assay system using a non-adherent cell line to evaluate the effect of a drug on *Toxoplasma gondii*. International Journal for Parasitology 25, 699–704.

Chang, H.R., Jefford, C.W., Peche're, J.-C., 1989. In vitro effects of three new 1,2,4-trioxanes (pentatroxane, thiahexatroxane, and hexatroxanone) on *Toxoplasma gondii*. Antimicrobial Agents and Chemotherapy 33, 1748–1752.

Chio, L.C., Queener, S.F., 1993. Identification of highly potent and selective inhibitors of *Toxoplasma gondii* dihydrofolate reductase. Antimicrobial Agents and Chemotherapy 37, 1914–1923.

Cory, A.H., Owen, J.C., Barltrop, J.A., Cory, J.G., 1991. Use of an aqueous soluble tetrazolium/formazan assay for cell growth assays in culture. Cancer Communications 3, 207–212.

Decker, T., Lohmann-Matthes, M.L., 1988. A quick and simple method for the quantitation of lactate dehydrogenase release in measurements of cellular cytotoxicity and tumor necrosis factor (TNF) activity. Journal of Immunological Methods 115, 61–69.

Derouin, F., Chastang, C., 1988. Enzyme immunoassay to assess effect of antimicrobial agents on *Toxoplasma gondii* in tissue culture. Antimicrobial Agents and Chemotherapy 32, 303–307.

Gay-Andrieu, F., Cozon, G.J., Ferrandiz, J., Kahi, S., Peyron, F., 1999. Flow cytometric quantification of *Toxoplasma gondii* cellular infection and replication. The Journal of Parasitology 85, 545–549.

Gubbels, M.J., Li, C., Striepen, B., 2003. High-throughput growth assay for *Toxoplasma gondii* using yellow fluorescent protein. Antimicrobial Agents and Chemotherapy 47, 309–316.

Haverkos, H.W., 1987. Assessment of therapy for toxoplasma encephalitis. The TE study group. The American Journal of Medicine 82, 907–914.

Holfels, E., McAuley, J., Mack, D., Milhous, W.K., McLeod, R., 1994. In vitro effects of artemisinin ether, cycloguanil hydrochloride (alone and in combination with sulfadiazine), quinine sulfate, mefloquine, primaquine, phosphate, trifluoperazine hydrochloride, and verapamil on *Toxoplasma gondii*. Antimicrobial Agents and Chemotherapy 38, 1392–1396.

Iltzsch, M.H., Uber, S.S., Tankersley, K.O., Kouni, M.H., 1995. Structure–activity relationship for the binding of nucleoside ligands to adenosine kinase from *Toxoplasma gondii*. Biochemical Pharmacology 49, 1501–1512.

Jones-Brando, L., D'Angelo, J., Posner, G.H., Yolken, R., 2006. In vitro inhibition of *Toxoplasma gondii* by four new derivatives of artemisinin. Antimicrobial Agents and Chemotherapy 50, 4206–4208.

Kamata, M., Ohta, M., Komatsu, K., Kim, H.-S., Wataya, Y., 2002. Synthesis, Fe(II)-induced degradation, and antimalarial activities of 1,5-diaryl-6,7-dioxabicyclo[3.2.2]nonanes: direct evidence for nucleophilic *O*-1,2-aryl shifts. Tetrahedron Letters 43, 2063–2067.

Korzeniewski, C., Callewaert, D.M., 1983. An enzyme-release assay for natural cytotoxicity. Journal of Immunological Methods 64, 313–320.

Mack, D.G., McLeod, R., 1984. New micromethod to study the effect of antimicrobial agents on *Toxoplasma gondii*: comparison of sulfadoxine and sulfadiazine individually and in combination with pyrimethamine and study of clindamycin, metronidazole, and cyclosporin A. Antimicrobial Agents and Chemotherapy 26, 26–30.

McFadden, D.C., Seeber, F., Boothroyd, J.C., 1997. Use of *Toxoplasma gondii* expressing beta-galactosidase for colorimetric assessment of drug activity in vitro. Antimicrobial Agents and Chemotherapy 41, 1849–1853.

Merli, A., Canessa, A., Melioli, G., 1985. Enzyme immunoassay for evaluation of *Toxoplasma gondii* growth in tissue culture. Journal of Clinical Microbiology 21, 88–91.

Meshnick, S.R., 2001. Artemisinin and its derivatives. In: Rosenthal, P.J. (Ed.), Antimalarial Chemotherapy: Mechanisms of Action, Resistance, and New Directions in Drug Discovery. Humana Press, Totowa, NJ, pp. 191–201.

Ou-Yang, K., Krug, E.C., Marr, J.J., Berens, R.L., 1990. Inhibition of growth of *Toxoplasma gondii* by qinghaosu and derivatives. Antimicrobial Agents and Chemotherapy 34, 1961–1965.

Pfefferkorn, E.R., Pfefferkorn, L.C., 1977. Specific labeling of intracellular *Toxoplasma gondii* with uracil. Journal of Protozoology 24, 449–453.

Pfefferkorn, E.R., Nothnagel, R.F., Borotz, S.E., 1992. Parasiticidal effect of clindameycin on *Toxoplasma gondii* grown in cultured cells and selection of a drug-resistant mutant. Antimicrobial Agents and Chemotherapy 36, 1091–1096.

Riss, T.L., Moravec, R.A., 1992. Comparison of MTT, XTT, and a novel tetrazolium compound for MTS for in vitro proliferation and chemosensitivity assays. Journal of Molecular Biology 3 (suppl.), 184a.

Tanaka, T., Omata, Y., Saito, A., Shimazaki, K., Yamauchi, K., Takase, M., Kawase, K., Igarashi, K., Suzuki, N., 1995. *Toxoplasma gondii*: parasiticidal effects of bovine lactoferricin against parasites. Experimental Parasitology 81, 614–617.

Symposium date: 27th September 2009

doi:10.1093/nass/nrp147

Association of nuclear-intermediate filament lamin B1 with necrotic- and apoptotic-morphologies in cell death Induced by 5-fluoro-2'-deoxyuridine

Akira Sato*, Akito Satake, Akiko Hiramoto, Akiko Okamatsu, Kentaro Nakama, Hye-Sook Kim and Yusuke Wataya

Faculty of Pharmaceutical Sciences, Okayama University, 1-1-1 Tsushimanaka, Kita-ku, Okayama 700-8530, Japan

ABSTRACT

We report that anticancer 5-fluoro-2'-deoxyuridine (FUdR) shows cytotoxicity against mouse cancer cell line FM3A cells, using a progeny clone F28-7 and its variant F28-7-A. In this process, the cell-death morphology is different between F28-7 and F28-7-A cells, that is, necrosis in F28-7 but apoptosis in F28-7-A cells. Recently we have investigated the gene and protein expression profiles of necrosis and apoptosis induced by FUdR using transcriptomic and proteomic analyses. In the proteomic analysis of these cells before their exposure to FUdR, the nuclear inner-membrane protein lamin B1 is up-regulated in F28-7 but not in F28-7-A, suggesting that lamin B1 may possess a function to regulate the morphology of cell-death. A knockdown of lamin B1 expression in F28-7 cells has now been performed by use of the small interfering RNA technique, resulting in a decrease of the lamin B1-expression level down to the level in F28-7-A. Remarkably, the FUdR-induced death morphology of this knocked-down F28-7 was apoptosis, definitely different from the necrosis that occurs in the FUdR-treated original F28-7. Our present finding provides an interesting possibility that lamin-B1 may have an important role in regulating cell-death morphology.

INTRODUCTION

Two general pathways for cell death have been defined, necrosis and apoptosis. Depending on cell type, cellular context, or stimulus, a cell is destined to necrosis or to apoptosis. Necrosis is characterized by swelling of the cell accompanying enlargement of the organelles in it, followed by disruption of the cell membrane, resulting in cell lysis. In contrast, apoptosis is morphologically characterized by membrane blebbing, shrinking of the cell and its organelles, and internucleosomal DNA degradation, followed by disintegration of the cell. However, previous studies of Leist and Nicotera[1], and Kakutani T., *et al.*[2] suggest that some early events in the death program may be common in the two types of cell death, and that downstream events may contribute to the guiding of cells towards necrosis or apoptosis. It is important to elucidate how a cell is guided toward either necrosis or apoptosis.

Recent studies indicate that signalling pathways, such as death receptors, kinase cascades, and mitochondria participate in both of these cell-death processes. We have now explored the possibility that by modulating these pathways, a switch between necrosis and apoptosis may occur.

5-Fluoro-2'-deoxyuridine (FUdR), a potent anticancer agent, exerts its effect by inhibiting thymidylate synthase, an essential machinery for DNA synthesis in cell proliferation[3, 4]. In our previous study on the action of FUdR against mouse mammary tumor FM3A cells, using the original clone F28-7 and its variant F28-7-A cells, we noticed that the FUdR-treatment can induce in F28-7 cells a breakdown of DNA into chromosome-sized fragments leading to necrosis, but, on the other hand, in F28-7-A a more extensive DNA cleavage into oligonucleosome-sized fragments and subsequent development of apoptosis[2]. Recently we reported the gene expression profiles of necrosis and apoptosis induced by FUdR and proposed possible mechanisms associated with the cell death in these sister cells[5]. Also we investigated the pattern of differentially expressed proteins in these cells by the proteomic analysis using two-dimensional gel electrophoresis and mass spectrometry. By an extensive proteomic analysis, it was found that the nuclear membrane-constituent protein lamin B1 is up-regulated in F28-7, while in F28-7-A cells its expression is at a normal level.

Here, we report that lamin B1 may regulate necrotic and apoptotic morphologies induced by FUdR. Thus, when a knockdown of lamin B1 expression in F28-7 cells by small interfering RNA (siRNA) was performed, the up-regulation of lamin B1 disappeared in these cells. We then explored whether this lack of up-regulation may affect the FUdR-induced cell-death morphology (see reference 6).

RESULTS AND DISCUSSION

In our proteomic analysis, lamin B1 was identified as an up-regulated protein in F28-7, in contrast to the normal level in the variant cell strain F28-7-A (unpublished data). Recent studies from several laboratories indicate that lamin

B1 and other lamins play a role in nuclear architecture, DNA replication, and gene expressions[7-11]. The possibility that lamin B1 may be associated with the differential patterns of cell death morphology observable in the treatment with FUdR is now investigated. To test if a down-regulation of endogenously expressed lamin B1 in F28-7 cells can modulate FUdR-induced necrosis, we carried out a knockdown of the expression in F28-7 cells by using lamin B1 siRNA. At 21 h after the treatment was initiated, the controls given vehicle or non-silencing siRNA showed the cytoplasmic swelling, a hallmark for necrosis. The lamin B1 siRNA transfected cells, in contrast, showed a typical apoptotic morphology; the membrane blebbing and the formation of apoptotic bodies (Fig. 1, at the bottom). In addition, non-silencing siRNA and lamin B1 siRNA themselves had no impact on the cell morphology, if no FUdR administration is performed (Fig. 1, upper diagram). These observations suggest that lamin B1 participates in modulating the process of necrosis and apoptosis. It would be important to further investigate the mechanisms involved in the lamin B1-control of the necrosis and apoptosis in the process of FUdR treatment.

CONCLUSION

We now revealed the possible association of nuclear-intermediate filament lamin B1 with necrosis and apoptosis in cell death induced by FUdR. Also, this finding suggests a new role for lamin B1 as a regulator in cell death. Our present work may contribute to the understanding of mechanisms regulating cell-death morphology.

REFERENCES

1. Leist, M., Nicotera, P. (1997) *Biochem. Biophys. Res. Commun.*, **236**, 1–9.
2. Kakutani, T., Ebara, Y., Kanja, K., Hidaka, M., Matsumoto, Y., Nagano, A., Wataya, Y. (1998) *Biochem. Biophys. Res. Commun.*, **247**, 773–779.
3. Santi, D. V. (1980) *J. Med. Chem.*, **23**, 103–111.
4. Yoshioka, A., Tanaka, S., Hiraoka, O., Koyama, Y., Hirota, Y., Ayusawa, D., Seno, T., Garrett, C., Wataya, Y. (1987) *J. Biol. Chem.*, **262**, 8235–8241.
5. Sato, A., Hiramoto, A., Uchikubo, Y., Miyazaki, E., Satake, A., Naito, T., Hiraoka, O., Miyake, T., Kim, H. S., Wataya, Y. (2008) *Genomics*, **92**, 9–17.
6. Sato, A., Hiramoto, A., Satake, A., Miyazaki, E., Naito, T., Wataya, Y., Kim, H. S. (2008) *Nucleosides, Nucleotides and Nucleic Acids*, **27**, 433–438.
7. Cohen, M., Lee, K. K., Wilson, K. L., Gruenbaum, Y. (2001) *Trends Biochem. Sci.*, **26**, 41–47.
8. Wilson, K. L., Zastrow, M. S., Lee, K. K. (2001) *Cell*, **104**, 647–650.
9. Goldman, R. D., Gruenbaum, Y., Moir, R. D., Shumaker, D. K., Spann, T. P. (2002) *Genes Dev.*, **16**, 533–547.
10. Burke, B., Stewart, C. L. (2002) *Nat. Rev. Mol. Cell Biol.*, **3**, 575–585.
11. Hutchison, C. J. (2002) *Nat. Rev. Mol. Cell Biol.*, **3**, 848–858.

*Corresponding author. E-mail: akirasat@cc.okayama-u.ac.jp

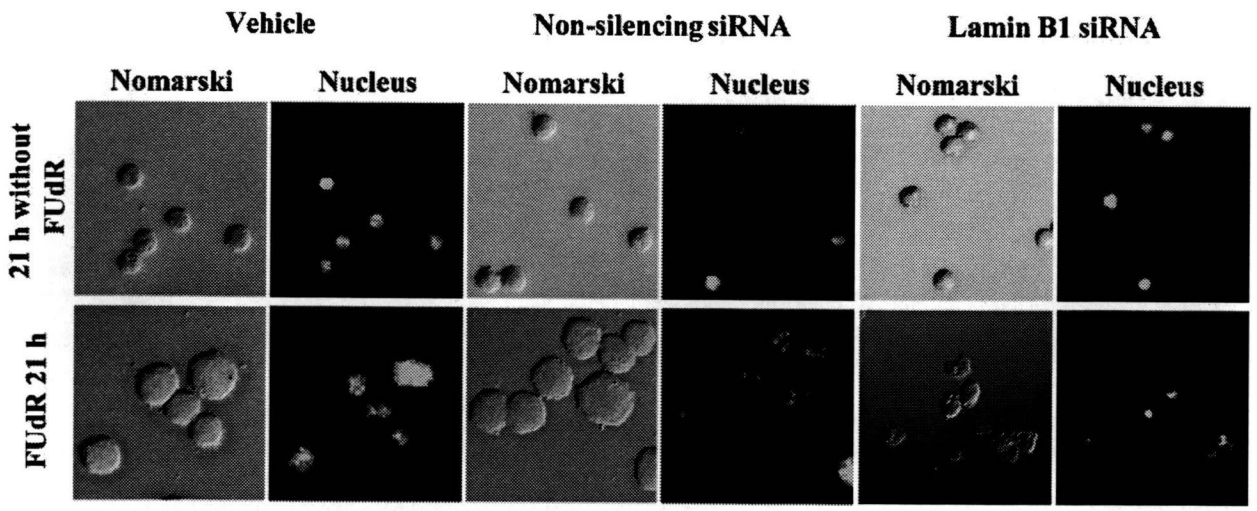

Fig. 1 Lamin B1 knockdown shifts FUdR-induced necrotic morphology to apoptotic morphology. Forty-eight hours after transfection with the vehicle, the non-silencing siRNA, or the lamin B1 siRNA, the F28-7 cells were treated with or without 1×10^{-6} M FUdR for 21 h and then stained with 4′, 6-diamidino-2-phenylindole dihydrochloride (DAPI). Morphological changes were analyzed under a fluorescence microscope at × 400 magnification.

Symposium date: 27th September 2009

doi:10.1093/nass/nrp146

Molecular mechanisms of apoptosis induced by 3'-ethynylcytidine

Yusuke Wataya[1]*, Tomoharu Naito[1], Akira Sato[1], Akiko Hiramoto[1], Yukio Kitade[2], Takuma Sasaki[3], Akira Matsuda[4], Masakazu Fukushima[5] and Hye-Sook Kim[1]

[1]Faculty of Pharmaceutical Sciences, Okayama University, 1-1-1 Tsushimanaka, Kita-ku, Okayama 700-8530, Japan, [2]Faculty of Engineering, Gifu University, 1-1 Yanagido, Gifu 501-1193, Japan, [3]School of Pharmacy, Aichi Gakuin University, 1-100 Kusumoto-cho, Chikusa-ku, Nagoya 464-8650, Japan, [4]Faculty of Pharmaceutical Sciences, Hokkaido University, Nishi 6, Kita 12, Kita-ku, Sapporo 060-0812, Japan, [5]Tokushima Research Center, Taiho Pharmaceutical Co., Ltd., 224-2 Hiraishi-ebisuno, Kawauchi-cho, Tokushima 771-0194, Japan

ABSTRACT

1-(3-*C*-Ethynyl-β-D-*ribo*-pentofuranosyl)cytosine (3'-Ethynylcytidine; ECyd), a ribonucleoside analog, has a potent cytotoxic activity against cancer cells. We have investigated the cancer-cell death induced by ECyd, focusing on its molecular mechanisms. In ECyd-treated cells, RNase L is activated and involved in c-jun NH_2-terminal kinase (JNK) phosphorylation, followed by induction of mitochondria-dependent apoptosis. The mechanism of JNK phophorylation by RNase L was unknown. To investigate the mechanism, we performed the identification of RNase L-binding partners by proteomic approach using co-immunoprecipitation and mass spectrometry. We found that RNase L was associated with a protein (we named it Protein-190). At the same time, we observed that Protein-190 was amply phosphorylated. Furthermore, the participation of Protein-190 in the ECyd-induced apoptosis was supported by a knockdown experiment using small interfering RNA (siRNA). Thus, the number of ECyd-induced apoptotic cells was drastically decreased when Protein-190 was knocked-down. These results indicated Protein-190 as a regulator in apoptosis, and provide the possibility for a new clinical target in cancer chemotherapy.

INTRODUCTION

1-(3-*C*-Ethynyl-β-D-*ribo*-pentofuranosyl)cytosine (3'-Ethynylcytidine; ECyd) is an RNA synthesis inhibitor through competitive inhibition of RNA polymerase I in nucleus. It induces 28S ribosomal RNA fragmentation in D8 domain. The fragmentation sites resembled those for RNase L-mediated cleavage sites. RNase L is an endoribonuclease that functions against viral infections and requires 5'-end-triphosphorylated-2', 5' oligoadenylates (2-5A) for its activity. Activation of RNase L by 2-5A leads to apoptosis[1-3]. The apoptosis-favoring activity of RNase L may restrict tumor growth as suggested by recent mapping of the hereditary prostate cancer 1 (*HPC1*) susceptibility allele to the RNase L gene[4, 5]. Activation of RNase L in cells leads to mitochondrial release of cytochrome *c* and caspase-dependent apoptosis[2]. Recently, it was demonstrated that the activation of RNase L leads to c-jun NH_2-terminal kinase (JNK) activation[6-8]. Apoptosis induced by 2-5A is defective in $JNK1^{-/-}JNK2^{-/-}$ mouse embryonic fibroblasts, thus implicating JNK in the apoptotic signal pathway initiated by RNase L activity[8]. RNase L is known to have specific affinities to various proteins[9-15].

Recently, we reported the role of RNase L in apoptosis induced by ECyd (see reference 16). Thus, RNase L is necessary for JNK phosphorylation and then induces mitochondria-dependent apoptosis. In this study, to investigate the mechanism of association with RNase L and JNK-mitochondrial signal pathway, we performed the identification of RNase L-binding partners using co-immunoprecipitation and Nano-LC-MS/MS system.

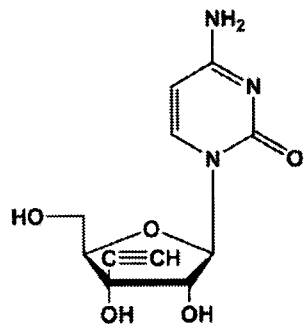

Fig. 1 Structure of 1-(3-*C*-Ethynyl-β-D-*ribo*-pentofuranosyl)cytosine

RESULTS AND DISCUSSION

In this study, we have found that RNase L is associated with Protein-190. The quantity of RNase-L=Protein-190 complex increased in response to the ECyd-treatment. In addition, Protein-190 had been phosphorylated in this complex. The levels of the complex formation and the phosphorylation were decreased by the knockdown of Protein-190 with siRNA-treatment. In addition, the number of ECyd-induced apoptotic cells was drastically

decreased when Protein-190 was knocked-down. These results indicate that phosphorylated Protein-190 is necessary to the RNase L-mediated apoptosis. However, the mechanism by which Protein-190 is associated with and phosphorylated by RNase L remains unclear. Although it is known that RNase L targets the proximal RNA substrates, RNase L could also be associated with other protein substrates, because the NH_2-terminal region of RNase L contains a series of nine ankyrin repeats which have been implicated in mediating protein-protein interactions[17]. Furthermore, RNase L also contains several protein kinase-like domains in which a conserved lysine residue that functions in the binding to phosphoryl groups of ATP is present[18, 19]. The presence of these functional domains indicates the possibility that RNase L binds to Protein-190 on ankyrin repeat domain(s) and phosphorylates Protein-190 by its protein kinase activity. Such a kinase activity, however, is yet to be detected.

These findings indicate that Protein-190 contributes to apoptosis induced by ECyd-treatment. Therefore, we suggest that the interaction(s) between RNase L and Protein-190 can play an important role for apoptotic signaling pathway, and together RNase L and Protein-190 function as apoptotic regulators for the downstream events of RNase L-dependent apoptotic pathway.

CONCLUSION

The results from this study demonstrated that RNase L is associated with Protein-190, and that the complex seems to play a role in the JNK-mitochondria dependent apoptosis-signaling pathway. We propose this new role for RNase L in the apoptotic mechanisms. These findings may open up the possibility of finding new targets for anticancer agents.

REFERENCES

1. Castelli, J. C., Hassel, B. A., Wood, K. A. *et al.* (1997) *J. Exp. Med.*, **18**, 967–972.
2. Rusch, L., Zhou, A., Silverman, R. H. (2000) *J. Interferon. Cytokine. Res.*, **20**, 1091–1100.
3. Zhou, A., Paranjape, J., Brown, T.L. *et al.* (1997) *EMBO J.*, **16**, 6355–6363.
4. Silverman, R. H. (2002) *Biochemistry*. **42**, 1805–1812.
5. Carpten, J., Nupponen, N., Isaacs, S. *et al.* (2002) *Nat. Genet.*, **30**, 181–184.
6. Iordanov, M. S., Pribnow, D., Magun, J. L. *et al.* (1997) *Mol. Cell. Biol.*, **17**, 3373–3381.
7. Iordanov, M. S., Paranjape, J. M., Zhou, A. *et al.* (2000) *Mol. Cell. Biol.*, **20**, 617–627.
8. Li, G., Xiang, Y., Sabapathy, K. *et al.* (2004) *J. Biol. Chem.*, **279**, 1123–1131.
9. Tanaka, N., Nakanishi, M., Kusakabe, Y. *et al.* (2004) *EMBO. J.*, **20**, 3929–3938.
10. Tanaka, N., Nakanishi, M., Kusakabe, Y. *et al.* (2005) *Protein. Rept. Lett.*, **12**, 387–389.
11. Dong, B., Silverman, R. H. (1997) *J. Biol. Chem.*, **272**, 22236–22242.
12. Sedwick, S. G., Smerdon, S. J. (1999) *Trends. Biochem. Sci.*, **24**, 311–316.
13. Dong, B., Niwa, M., Walter, P. *et al.* (2001) *RNA*, **7**, 361–373.
14. Le, R.F., Salehzada, T., Bisbal, C. *et al.* (2005) *Nat. Struct. Mol. Biol.*, **12**, 505–512.
15. Bettoun, D. J., Scafonas, A., Rutledge, S. J. *et al.* (2005) *J. Biol. Chem.*, **280**, 38898–38901.
16. Naito, T., Yokogawa, T., Takatori, S. *et al.* (2009) *Cancer Chemother. Pharmacol.*, **63**, 837–850.
17. Foord, R. (1999) *Nat. Struct. Biol.*, **6**, 157–165.
18. Hank, S. K., Quinn, A. M., Hunter, T. (1998) *Science*, **241**, 42–52.
19. Taylor, S.S., Knighton, D. R., Zheng, J. *et al.* (1992) *Ann. Rev. Cell. Biol.*, **8**, 429–462.

*Corresponding author. E-mail:
wataya@cc.okayama-u.ac.jp

FULL PAPER *Parasitology*

Evaluation of Efficacy of Bruceine A, a Natural Quassinoid Compound Extracted from a Medicinal Plant, *Brucea javanica*, for Canine Babesiosis

Ryo NAKAO[1], Chiaki MIZUKAMI[1], Yuta KAWAMURA[1], SUBEKI[1], Saw BAWM[1], Masahiro YAMASAKI[2], Yoshimitsu MAEDE[2], Hideyuki MATSUURA[3], Kensuke NABETA[3], Nariaki NONAKA[1], Yuzaburo OKU[1] and Ken KATAKURA[1]*

[1]*Laboratory of Parasitology, Department of Disease Control,* [2]*Laboratory of Internal Medicine, Department of Veterinary Clinical Science, Graduate School of Veterinary Medicine, Hokkaido University, Kita 18, Nishi 9, Kita-ku, Sapporo 060–0818 and* [3]*Laboratory of Bioorganic Chemistry, Division of Applied Life Science, Graduate School of Agriculture, Hokkaido University, Kita 9, Nishi 9, Kita-ku, Sapporo 060–8589, Japan*

(Received 30 June 2008/Accepted 25 August 2008)

ABSTRACT. Bruceine A, a natural quassinoid compound extracted from the dried fruits of *Brucea javanica* (L.) Merr., was evaluated for its antibabesial activity *in vitro* and *in vivo*. Bruceine A inhibited the *in vitro* growth of *Babesia gibsoni* in canine erythrocytes at lower concentration compared with the standard antibabesial drug diminazene aceturate and killed the parasites within 24 hr at a concentration of 25 *n*M. Oral administration of bruceine A at a dosage of 6.4 mg/kg/day for 5 days resulted in no clinical findings in a dog with normal ranges of hematological and biochemical values in the blood. Three dogs were infected with *B. gibsoni* and two of them were treated with bruceine A at a dosage of 6.4 mg/kg/day for 6 days from day 5 post-infection. An untreated dog developed typical acute babesiosis symptoms including severe anemia, high fever, and complete loss of appetite and movement. However, the two bruceine A-treated dogs maintained their healthy conditions throughout the experimental period of 4 weeks although complete elimination of parasites from the peripheral blood was not achieved and decreases in the packed cell volume and the erythrocyte and platelet counts were observed. Since natural quassinoid compounds have been used as traditional medicines for the treatment of various ailments including cancer and malaria, the present results suggest that bruceine A or other related compounds are potential candidates for the treatment of canine babesiosis.
KEY WORDS: *Babesia gibsoni*, *Brucea javanica*, Bruceine A, Chemotherapy, Medicinal plant.

J. Vet. Med. Sci. 71(1): 33–41, 2009

Canine babesiosis is a tick-borne disease caused by the intraerythrocytic apicomplexan parasites, *Babesia gibsoni* and *B. canis*. Clinical signs of *B. gibsoni* infection are anemia, fever, thrombocytopenia, splenomegaly, lymphadenopathy, and lethargy [19]. During the acute phase of infection, infected dogs develop severe anemia and occasionally die if adequate treatment is not provided. However, most dogs that recovered from the acute phase become carriers of the parasites and may suffer from disease relapses for the rest of their life. *B. gibsoni* infection is endemic in many regions in Asia, Africa, Europe, Australia, Brazil, and North America [4, 10]. In Japan, *B. gibsoni* infection has long been problematic especially in western regions, but recently the distribution appears to be expanding to the eastern parts of Japan [21].

Diminazene aceturate and imidocarb dipropionate are the major drugs for the treatment of *B. gibsoni* infection [16], but these drugs are unable to eliminate the parasites completely from infected dogs [30]. These drugs also have some disadvantages. The toxicity of diminazene aceturate to kidney, brain, and liver can result in serious side-effects such as weakness, irritability, paralysis, lack of responsiveness to stimuli, and fatal hemorrhage in the central nervous system [20, 26]. Due to these side-effects, the practical use of diminazene aceturate is not approved by the Food and Drug Administration (FDA) in the U.S.A. [5], and this drug was recently withdrawn from the market in Japan. The limited use of imidocarb dipropionate may be due to its high cost and systemic side-effects such as acute hepatic and renal failure especially in debilitated animals [1]. Therefore, an alternative chemotherapeutic agent with better activity and fewer side-effects is needed urgently. One possible source of such affordable treatment lies in the use of medicinal plants.

In the preceding study [24], Indonesian medicinal plants were screened for antibabesial activity *in vitro* and active quassinoid compounds were extracted from the fruit of *Brucea javanica* (L.) Merr., a plant species of the family Simaroubaceae. This plant contained a number of quassinoids as the bitter principles. Among these quassinoids, bruceine A, bruceantinol, and bruceine C showed sufficient antibabesial activities. The 50% growth-inhibitory concentration (IC_{50}) values were 4 *n*g/ml (7.7 *n*M), 12 *n*g/ml (19.8 *n*M), and 107 *n*g/ml (189.7 *n*M), respectively, which compared well with the standard drug, diminazene aceturate, having an IC_{50} value of 103 *n*g/ml (172.6 *n*M).

The present study was examined on the effect of bruceine A against *B. gibsoni in vitro* in more detail and evaluated the efficacy of bruceine A for dogs at an early stage of infection with *B. gibsoni* by investigating their clinical signs, the level of parasitemia, and hematological and biochemical values in

* CORRESPONDENCE TO: KATAKURA, K., Laboratory of Parasitology, Department of Disease Control, Graduate School of Veterinary Medicine, Hokkaido University, Kita 18, Nishi 9, Kita-ku, Sapporo 060–0818, Japan.
e-mail: kenkata@vetmed.hokudai.ac.jp

the blood. The amount of parasite DNA in the peripheral blood was also monitored using a real-time polymerase chain reaction (PCR) method as a new assessment of antibabesial chemotherapeutics.

MATERIALS AND METHODS

Preparation of bruceine A: The dried fruits of *Brucea javanica* were purchased from Bandar Jaya traditional market, Lampung, Indonesia, in April 2005. The plant species was identified by Mr. Aris Winarso at the Herbal Medicine Research and Education Centre, Lampung, Indonesia. Extraction and purification of bruceine A was described in the previous paper [24]. Briefly, air dried fruits (1 kg) were boiled with 5 *l* of water for 30 min twice. The boiling water was filtered and extracted with ethyl acetate (EtOAc) to give aqueous and EtOAc fractions. The EtOAc fraction was filtered, evaporated, and chromatographed on a silica gel column with chloroform, methanol (MeOH)-chloroform (3:97, 2*l*), MeOH-chloroform (1:4, 2*l*), MeOH-chloroform (7:3, 2*l*), and MeOH, successively. Each fraction was tested for its antibabesial activity against *B. gibsoni*. The active fraction was then chromatographed on a silica gel column with hexane-EtOAc (1:1) to give ten fractions. Bruceine A was detected in the fifth fraction and crystallized using MeOH. The structure was determined by means of NMR and mass spectra.

Parasites: The strain of *B. gibsoni* used was originally isolated from a naturally infected dog in Nagasaki Pref. in 1973 and has been maintained in dogs at Hokkaido University since then. The parasites were also maintained in 24-well plates (Corning, Corning, NY, U.S.A.) at 37°C with a gas flow mixture composed of 5% CO_2, 5% O_2, and 90% N_2. Approximately 60% of the culture supernatant was replaced daily with an equal volume of fresh medium. Every 7 days, a half volume of erythrocyte suspension was replaced with the same volume of uninfected erythrocyte suspension.

Preparation of canine erythrocyte suspension: Canine erythrocytes were prepared by the method of Yamasaki *et al.* [34] with some modifications. Venous blood was collected from the jugular vein of healthy adult dogs. The erythrocytes were washed three times in a modified Vega y Martinez phosphate-buffered saline solution (mVYM) [29] by centrifugation at 1,200 × g for 5 min at 4°C. After two additional washes with RPMI-1640 (Gibco, Invitrogen Co., CA, U.S.A.) medium, the cells were resuspended in RPMI-1640 supplemented with 0.1 mg/m*l* sodium pyruvate (Wako, Osaka, Japan), 0.3 mg/m*l* L-glutamine (Wako, Osaka, Japan), 2 mg/m*l* sodium bicarbonate (Wako, Osaka, Japan), 100 units/m*l* penicillin G potassium (Meiji Seika, Tokyo, Japan), and 20% (v/v) heat-inactivated dog serum to yield a packed cell volume (PCV) of 5%.

Assay for in vitro antibabesial activity of bruceine A: Bruceine A and diminazene aceturate (Hoechst AG, Germany) were dissolved in DMSO and kept in the dark at 4°C until use. The stock solution was diluted with culture medium containing 0.1% DMSO. *B. gibsoni*-infected erythrocytes (approximately 1% parasitemia) were obtained by diluting the cultures (5.0–6.5% parasitemia) with non-infected erythrocyte suspension. To each well of a 24-well culture plate a volume of 500 μl infected erythrocyte suspension was added. After settling, a 50 μl aliquot of the supernatant was removed and 50 μl of bruceine A solution was added to give final concentrations of 0, 6.3, 12.5, 25, 50, and 100 *n*M. The plate was incubated at 37°C with a gas flow mixture composed of 5% CO_2, 5% O_2, and 90% N_2 for 7 days. Approximately 60% of the supernatant was removed and replaced every 24 hr with fresh medium containing bruceine A at the appropriate concentration. Diminazene aceturate was used at concentrations of 0, 50, 100, 400, and 1,600 *n*M. Every 24 hr, 10 μl of the erythrocyte suspension was sampled from each well and mixed with 90 μl of phosphate buffered saline (PBS). The mixture was centrifuged and attached to a slide using a cytocentrifuge (Shandon Cytospin 2; Shandon, Cheshire, England) for 5 min at 450 rpm. The slide was fixed with methanol and stained with Giemsa solution (pH 7.4). The parasitemia level was determined by counting the number of parasitized erythrocytes in 2,000 erythrocytes. When the parasitemia level was less than 1%, an additional 3,000 erythrocytes were examined. The experiment was carried out in triplicate. Statistical analysis was carried out using Student's *t*-test.

Assay for antibabesial activity of bruceine A in dogs: Four beagle dogs (10-month-old, male) were used in this study. All experiments were conducted in accordance with the Guidelines for the Care and Use of Laboratory Animals of Hokkaido University. One dog (dog A) was used to examine the side-effects of bruceine A and received a gelatin capsule containing bruceine A powder orally at dosages of 0.4, 0.8, 1.6, 3.2, and 6.4 mg/kg at 24 hr intervals. Since no acute toxicity was observed at any dosage, the same dog was administered bruceine A at an oral dosage of 6.4 mg/kg for 5 days at 24 hr intervals. Thus, dog A received bruceine A at a total dosage of 44.4 mg/kg. Clinical findings, body weight, and body temperature were monitored. Peripheral blood (5 m*l*) was collected and subjected to hematological and biochemical examinations. Packed cell volume (PCV), red blood cell counts, and platelet counts were measured using an automatic cell counter (Celltac-α, MEK-6258; Nihon Kohden, Tokyo, Japan). Serum biochemical parameters such as alkaline phosphatase (ALP), alanine aminotransferase (ALT), aspartate aminotransferase (AST), blood urea nitrogen (BUN), creatinine (CRE), gamma-glutamyl transpeptidase (GGT), glucose (GLU), and total cholesterol (TCHO) were measured using an analyzer (DRI-CHEM 7000V; Fuji Mechanical Industry Co., Ltd., Tokyo, Japan), and serum levels of electrolytes (Na^+, K^+, and Cl^-) were measured with an ion-selective electrode (Dri-Chem Slide Na-K-Cl; Dri-Chem 800 V; Fuji Film Co., Ltd., Tokyo, Japan).

Three dogs (dogs B, C, and D) were inoculated intravenously with 1.2×10^9 *B. gibsoni*-parasitized erythrocytes in a volume of 9 m*l*, which were harvested from a dog chroni-

cally infected with *B. gibsoni*. Bruceine A in a gelatin capsule was administered to two dogs (dogs B and C) at an oral dosage of 6.4 mg/kg/day for 6 days (a total dosage of 38.4 mg/kg) starting from day 5 post-infection. Dog D was served as the control and administered a gelatin capsule containing glucose powder. Clinical findings and body temperature were monitored for the experimental period of 28 days. Peripheral blood (500 μl) was collected daily and a 200 μl volume of each blood sample was subjected to hematological, biochemical, and microscopic examinations as described above. The rest of the blood sample was stored at –20°C until use for real-time PCR assays. Hematological examinations were conducted daily, while serum biochemical examinations were performed on days 0, 4, 11, 18, and 25 post-infection. Blood smears were made from EDTA-anticoagulated peripheral blood samples and stained with Giemsa solution. The level of parasitemia was determined by counting 10,000 erythrocytes.

Quantification of B. gibsoni p18 gene in the blood by real-time PCR: The copy number of the *B. gibsoni* p18 gene in the peripheral blood was estimated using the real-time PCR method by Matsuu *et al.* [18]. DNA was extracted from 200 μl of EDTA-anticoagulated whole blood samples using a commercial kit (QIAgen DNA Blood Mini Kit; Qiagen, Tokyo, Japan). Real-time PCR assays were performed with a reaction mixture (25 μl) containing each primer (500 *n*M) and template DNA extract (0.5 μl) using an Applied Biosystems 7300 real-time PCR System (Applied Biosystems, Foster City, CA, U.S.A.) and Power SYBR Green PCR Master Mix (Applied Biosystems, Tokyo, Japan). The mixture was incubated at 50°C for 2 min and 95°C for 10 min, followed by 40 cycles of 95°C for 15 s and 60°C for 60 s. The relative copy number of the p18 gene in the blood samples was estimated from a standard curve created by plotting the log initial copy number of input plasmid, which contains a 182-base pair fragment of the p18 target gene, against the threshold cycle (Ct) value. Each sample was measured in triplicate and the results were expressed as the copy number per 100 erythrocytes (mean ± SD).

RESULTS

In vitro antibabesial activity of bruceine A: The kinetics of parasitemia in the canine erythrocytes with *B. gibsoni* in culture for 7 days is shown in Fig. 1. While previous report showed that bruceine A had an IC_{50} value of 4 *n*g/m*l* (7.7 *n*M) against the parasites at day 3 of the culture [24], a similar result was obtained at day 3 in this study, in which the level of parasitemia for the untreated culture and the culture treated with 6.3 *n*M bruceine A was 3 and 1.6%, respectively (Fig. 1-A, inset). Thus, bruceine A at 6.3 *n*M inhibited parasite growth by 47% at day 3 of the culture. Although parasitemia reached 12% at day 7 in the drug-free culture, it remained around 3% in the culture in the presence of 6.3 *n*M bruceine A, indicating that complete growth inhibition was not obtained at this concentration of the drug. On the other hand, parasitemia levels rapidly decreased within one day with 25 *n*M bruceine A, (Fig. 1-A, inset) and some morphological abnormalities of the parasites including a pyknosis-like and comma-shaped changes were observed (data not shown). Similar results of rapid decrease in parasitemia and morphological changes of the parasites were observed in the presence of 50 and 100 *n*M bruceine A (data not shown). However, no such rapid reduction in parasitemia was observed with the standard antibabesial drug, diminazene aceturate, even at the highest concentration of 1,600 *n*M (Fig. 1-B).

In vivo effect of bruceine A on B. gibsoni-infected dogs: One dog (dog A) was used to the examination for the side-effects of bruceine A and received this compound orally in a gelatin capsule at a dosage of 6.4 mg/kg/day for 5 days. No serious clinical findings were found in this dog. Hematological and serum biochemical values including PCV, red blood cell counts, platelet counts, ALP, ALT, AST, BUN, CRE, GGT, GLU, TCHO, and electrolytes (Na^+, K^+, and Cl^-) were all within respective reference range (data not shown).

Three dogs were then infected with *B. gibsoni*. Two of them (dogs B and C) were administered 6.4 mg/kg/day bruceine A orally for 6 days from day 5 post-infection, and the other one (dog D) was kept untreated. The kinetics of parasitemia and body temperature in these dogs is shown in Fig. 2. In the untreated dog D a gradual rise in parasitemia was observed and the value reached a peak of 2.3% on day 13 (Fig. 2, Dog D). This dog showed severe pallor in the mucous membranes from day 12 and its body temperature began to rise from day 8 and rose to 40.4°C on day 14 (Fig. 2, Dog D). The dog exhibited complete loss of appetite and movement on day 13 and reached the humane endpoint (*f* in Fig 2, Dog D) on day 14 before receiving a subcutaneous infusion to prevent lasting harm. Bruceine A-treated dogs (dogs B and C) also showed a gradual increase in parasitemia levels until day 11, but there were no obvious peaks and the levels were kept below 1% during the experimental period (Fig. 2, Dogs B and C). Dog B did not show any clinical signs. Dog C showed pallor in the mucous membranes from day 13 for 4 days and developed high fever sporadically on days 14 and 15. Anorexia and depression were, however, not observed in these bruceine A-treated dogs.

The kinetics of PCV and platelet counts is shown in Fig. 3. In dog B the PCV level decreased gradually but it was maintained at over 28% (Fig. 3, Dog B). The PCV in dog C decreased markedly and reached nadir values of 18% on day 15, and 15% (the humane endpoint in this experiment) in dog D on day 14, respectively (Fig. 3, Dogs C and D). However, in dog C the level recovered and was maintained at around 30 to 40%. The decrease in erythrocyte counts was associated with the decrease in PCV values in each dog (data not shown). A drastic decrease in platelet counts was observed in these dogs. Although the respective dogs had about 300,000/μl platelets in the blood before infection, they contained less than 10,000/μl on day 14 (Fig. 3, Dogs B, C, and D). Dog B maintained platelet counts at a lower

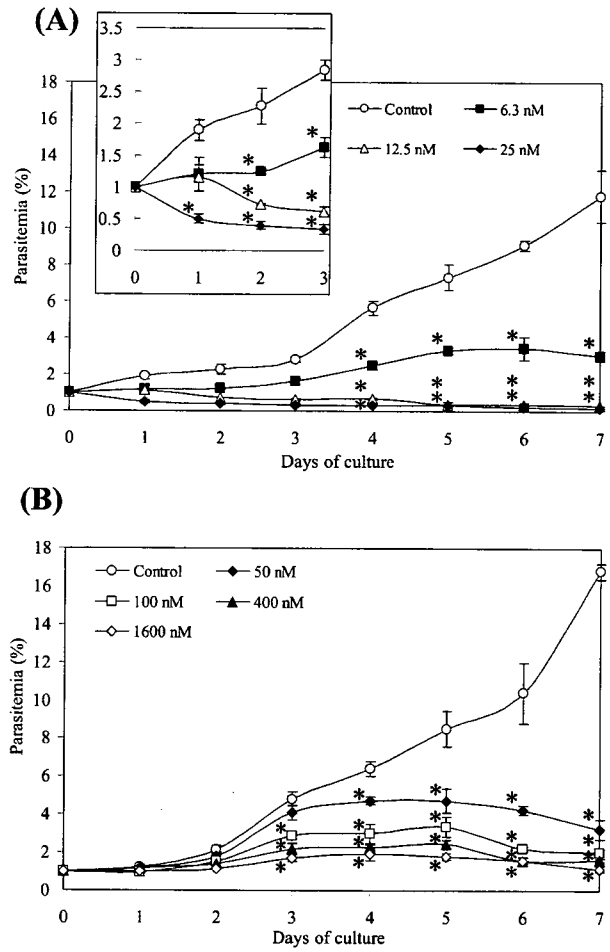

Fig. 1. Growth of *Babesia gibsoni* in the canine erythrocytes *in vitro* in the presence of bruceine A (A) and diminazene aceturate (B). Every 24 hr, each culture suspension was sampled and parasitemia was determined. Data show the means ± SD of two separate experiments. Insert indicates an expanded view of the growth curves for the initial 3 days in the presence of bruceine A. The asterisk (*) indicates statistically significant difference at $p<0.01$ from the control values by Student's *t*-test.

level of less than 55,000/μl during the experimental period. In dog C, the platelet counts increased to a normal level (240,000/μl) on day 21 but then decreased again.

With respect to serum biochemical values and serum levels of electrolytes, only the ALT value (136 U/*l*) in dog B on day 4 exceeded the reference value (17–78 U/*l*), whereas all other parameters were within each reference range (data not shown).

Detection of B. gibsoni p18 gene in the blood: The kinetics of the p18 gene copy number and parasitemia in the dogs is shown in Fig. 4. Parasite DNA was detected in the peripheral blood from day 1 and the p18 gene copy number reached a first peak on day 11, showing 4.3, 8.0, and 7.0 copies/100 erythrocytes in dogs B, C, and D, respectively (Fig. 4). The copy number decreased subsequently in all three dogs but then gradually increased again in dogs B and C.

DISCUSSION

This study showed that bruceine A had potent antibabesial activities against *B. gibsoni in vitro* and *in vivo*. The *in vitro* results indicated that a rapid decrease in parasitemia was induced by bruceine A at a concentration of 25 *n*M, suggesting that the parasites were killed at this concentration. The oral administration of bruceine A to dogs at an early

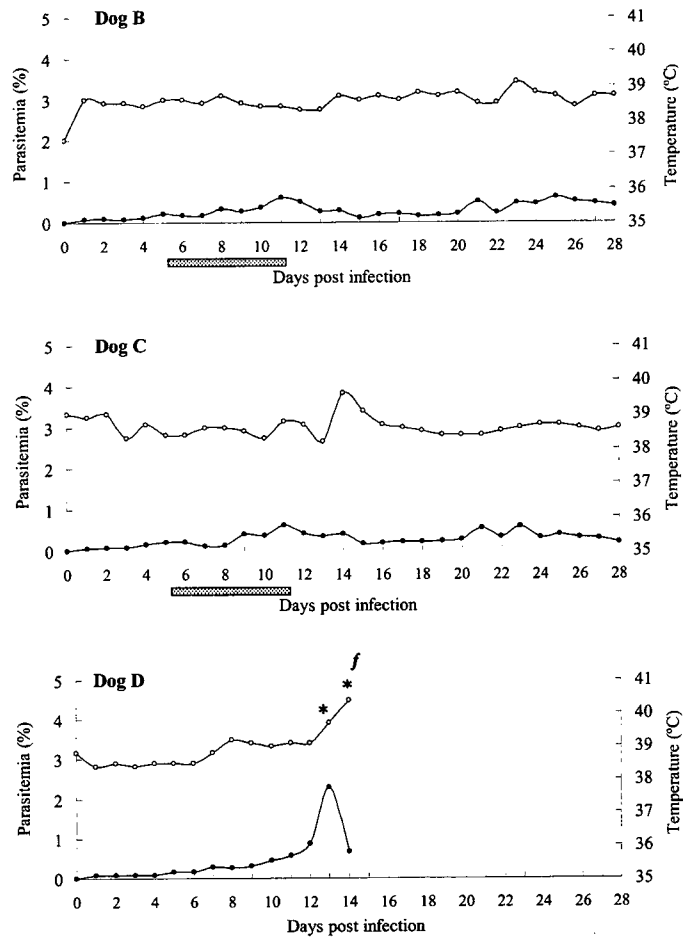

Fig. 2. Changes in parasitemia (-●-) and body temperature (-○-) in the dogs (B, C, and D) infected with *Babesia gibsoni*. Dogs B and C were administered bruceine A (6.4 mg/kg/day) orally from day 5 post-infection for 6 days. The dark grey bars indicate the period of bruceine A administration. Untreated dog D showed complete loss of appetite and movement (*) and reached humane end-point (*f*).

stage of infection with *B. gibsoni* relieved some of the clinical signs of infected dogs. An untreated dog developed severe anemia, high fever, and complete loss of appetite and movement, whereas two bruceine A-treated dogs maintained healthy conditions. However, in these treated dogs decreases in PCV value and erythrocyte and platelet counts were observed and complete elimination of the parasites from the peripheral blood was not achievable. These results suggested that bruceine A inhibited the growth of parasites to a certain extent and prevented the manifestation of clinical signs associated with *B. gibsoni* infection in dogs.

It is reported that the degree of thrombocytopenia is more severe than that of anemia in *B. gibsoni*-infected dogs [9, 11, 17, 33]. This clinical finding was also observed in the present study. Dog C showed a temporal recovery from thrombocytopenia from day 15, however, this may not be related to the drug treatment since dog B did not show a similar recovery. Treatment with atovaquone alone, atovaquone in combination with azithromycin, and clindamycin alone against *B. gibsoni*-infected dogs has been reported to show a rapid decrease in parasitemia and significant improvement of clinical findings including anemia and thrombocyteopenia, in spite of unsuccess in total elimination of circulating parasites [11, 17, 33]. Unlike *in vitro* results, a rapid elimination of the parasites in the peripheral erythrocytes was not observed in the infected dogs by treatment with bruceine A in the present study. Since sequestration of *B. gibsoni*-infected erythrocytes within the tissues such as the lymph node and spleen has been suggested [11, 17], bruceine A might inhibit the growth of parasites in the